AEDC-TR-73-170.

Cy. 2

DESIGN ASSURANCE TEST OF THE THIOKOL TE-M-521-5 APOGEE KICK MOTOR TESTED IN THE SPIN MODE AT SIMULATED ALTITUDE CONDITIONS

J. O. Brooks and H. L. Merryman

ARO, Inc.

November 1973

Approved for public release; distribution unlimited.

ENGINE TEST FACILITY
ARNOLD ENGINEERING DEVELOPMENT CENTER
AIR FORCE SYSTEMS COMMAND
ARNOLD AIR FORCE STATION, TENNESSEE

NOTICES

DESIGN ASSURANCE TEST OF THE THIOKOL TE-M-521-5 APOGEE KICK MOTOR TESTED IN THE SPIN MODE AT SIMULATED ALTITUDE CONDITIONS

J. O. Brooks and H. L. Merryman
ARO, Inc.

FOREWORD

The test program reported herein was conducted at the Arnold Engineering Development Center (AEDC), Air Force Systems Command (AFSC), under the sponsorship of the National Aeronautics and Space Administration (NASA), Goddard Space Flight Center (GSFC), for the Thiokol Chemical Corporation (TCC), Elkton Division, under Program Element 921E3.

The results of the test were obtained by ARO, Inc. (a subsidiary of Sverdrup & Parcel and Associates, Inc.), contract operator of the AEDC, AFSC, Arnold Air Force Station, Tennessee. The test was conducted in Propulsion Development Test Cell (T-3) of the Engine Test Facility (ETF) on June 1, 1973, under ARO Project No. RA294, and the manuscript was submitted for publication on September 6, 1973.

This technical report has been reviewed and is approved.

CHAUNCEY D. SMITH, JR.
Lt Colonel, USAF
Chief Air Force Test Director, ETF
Directorate of Test

FRANK J. PASSARELLO
Colonel, USAF
Director of Test

ABSTRACT

One Thiokol Chemical Corporation TE-M-521-5 solid-propellant apogee rocket motor was successfully fired at an average simulated altitude of about 103,000 ft while spinning at 46 rpm. The general program objectives were to verify compliance of motor performance with the manufacturer's specifications. Specific primary objectives were to determine vacuum ballistic performance of the motor after prefire vibration conditioning and temperature conditioning at 40°F, altitude ignition characteristics, motor structural integrity, and motor temperature-time history during and after motor operation. Additional objectives were to measure the lateral (nonaxial) thrust component during motor operation and to measure radiation heat flux in the vicinity of the nozzle exit plane.

CONTENTS

APPENDIXES

NOMENCLATURE

A_{ex}	Nozzle exit area, in.^{2}
A_t	Nozzle throat area, in.^{2}
$\overline{C}_f$	Average vacuum thrust coefficient over a selected 1-sec interval of motor operation just prior to tailoff
F	Measured axial thrust, lbf
$I_{vac_{action}}$	Vacuum impulse based on action time (t_a), lbf-sec
$I_{vac_{total}}$	Vacuum impulse based on total burn time (t_{is}), lbf-sec
P_{cell}	Measured cell pressure, psia
P_{ch}	Measured chamber pressure, psia
t_a	Action time, time interval from 10 percent of maximum chamber pressure at ignition to 10 percent of maximum chamber pressure at tailoff, sec
t_{bd}	Time of nozzle flow breakdown, sec

t_{is}	Total burn time, time interval between the application of ignition voltage and the time at which the ratio of P_{ch} to P_{cell} has decreased to 1.3 during tailoff, sec
t_{ℓ}	Ignition lag time, time interval from application of ignition voltage to the first perceptible rise in chamber pressure, sec
t_o	Zero time, time of application of voltage to the igniter, sec

SECTION I
INTRODUCTION

The Thiokol Chemical Corporation (TCC) TE-M-521-5 solid-propellant rocket motor is to be used as the apogee kick motor for the Interplanetary Monitoring Platform (IMP)-H and -J spacecraft (Ref. 1). The kick motor will impart sufficient velocity to inject the spacecraft into a circular orbit at the apogee of its ascent transfer ellipse. The apogee motor is contained within the spacecraft, which is internally insulated to protect the communications package from the high temperatures attributable to apogee motor heat soakback (Ref. 1).

The test reported herein was a continuation of the design assurance test program for the TE-M-521-5 motor. Two TE-M-521-5 motors were previously tested at the AEDC (Refs. 2 and 3). The motor reported herein differed from the motors reported in Refs. 2 and 3 in that the aft pressure relief boot had been modified (see Section 2.1).

The general objective of the test program reported herein was to verify compliance of motor performance to the manufacturer's specification (Ref. 4). Specific objectives were to determine: (1) the altitude ballistic performance of the TE-M-521-5 rocket motor while spinning about its axial centerline at 46 rpm after prefire vibration conditioning and temperature conditioning at 40 ± 5°F for a minimum of 24 hr; (2) altitude ignition characteristics; (3) motor structural integrity; and (4) motor temperature-time history during and after motor operation. Secondary objectives were to measure the lateral (nonaxial) thrust component during motor operation and to measure radiation heat flux in the vicinity of the nozzle exit plane.

Motor altitude ballistic performance, ignition characteristics, structural integrity, motor temperature, exhaust plume heat flux, and motor lateral (nonaxial) thrust are presented and discussed.

The TE-M-521-5 motor is ballistically identical to the earlier models of the TE-M-521 apogee kick motor, used for the Interim Defense Communication Satellite Program (IDCSP/A) spacecraft; however, the TE-M-521-5 has a greater minimum wall thickness specification (0.038 in. instead of 0.032 in.) in the forward and aft hemispheres, the nozzle exit cone is fabricated with an additional 0.050-in. phenolic glass cloth overwrap extending 5 in. downstream from the throat, and the Gengard V-44 rubber asbestos propellant-to-case insulation has been replaced with TIR-300 asbestos-polyisoprene.

SECTION II
APPARATUS

2.1 TEST ARTICLE

The Thiokol Chemical Corporation (TCC) TE-M-521-5 solid-propellant rocket motor (Fig. 1, Appendix I) is a full-scale, flightweight motor having the following nominal dimensions and burning characteristics at 40°F:

Length, in.	38.64
Diameter, in.	17.44
Loaded Weight, lbm	276
Propellant Weight, lbm	247
Maximum Thrust, lbf	4,200
Maximum Chamber Pressure, psia	780
Action Time, sec	20.0
Throat Area, in.^{2}	2.788
Nozzle Area Ratio, A_{ex}/A_t	53.5

The elongated spherical motor case is constructed of 0.071-in. forged titanium (6A1-4V) welded to two hemispherical sections of 0.038 in. thickness. The case is lined internally with TCC TL-H-304 liner and insulated with TIR-300 asbestos-polyisoprene. A stress relief boot assembly is contained in the forward and aft ends of the motor case (Fig. 1a). A flange around the motor cylindrical section provides for attachment to the IMP spacecraft.

Previous TE-M-521-5 motors (Refs. 2 and 3) utilized a stress relief boot extending from the igniter port to a position about 2 in. aft of the case midpoint (Fig. 1). Investigation by the manufacturer revealed a possibility that, during ignition, the part of the relief boot aft of the grain surface could seal against the primary insulator and cause a propellant-to-boot bond failure. For the motor reported herein, the relief boot was trimmed back from the igniter port to within 0.3 in. of the aft propellant surface (Fig. 1c).

The contoured nozzle assembly contains a Graph-I-Tite® G-90 carbon throat insert pinned and bonded to the nozzle adapter flange. The expansion cone is constructed of vitreous silica phenolic, externally coated with vapor-deposited aluminum. The cone is threaded, bonded, and pinned to the aluminum nozzle adapter flange. The nozzle assembly has a nominal 53.5:1 area ratio and a 14-deg half-angle at the exit plane. A Styrofoam® closure was bonded in the nozzle expansion cone. The closure was punctured prior to testing so that the rocket motor chamber pressure was equal to the simulated altitude pressure at motor ignition.

The TE-M-521-5 rocket motor contains a composite propellant grain formulation designated TP-H-3062 (ICC Class B), cast in an eight-point-star configuration.

Ignition was accomplished by igniting one of the two TE-P-386-7 pyrogen igniters (Fig. 1a) which incorporated Holex 4497 initiators and contained 20 $BKNO_3$ pellets (size 2A) used to initiate the 0.08-lbm primary polysulphide igniter grain. Nominal ignition current was 4.5 amp for 25 msec for the igniter.

2.2 INSTALLATION

The motor assembly was cantilever mounted from the spindle face of a spin-fixture assembly in Propulsion Development Test Cell (T-3). The spin assembly was mounted on a thrust cradle, which was supported from the cradle support stand by three vertical and two horizontal double-flexure columns (Fig. 2). The spin-fixture assembly consists of a 10-hp squirrel-cage-type drive motor, a thrust bearing assembly, a 46-in.-long spindle having a 36-in.-diam aft spindle face, and a 170-channel slip-ring assembly. The spin fixture rotated counterclockwise, looking upstream. Electrical leads to and from the igniters, pressure transducers, and thermocouples on the rotating motor were provided through a 170-channel, slip-ring assembly mounted between the forward and aft bearing assemblies of the spindle. Axial thrust was transmitted through the spindle thrust bearing assembly to two load cells mounted just forward of the thrust bearing on the motor axial centerline.

Preignition pressure altitude conditions were maintained in the test cell by a steam ejector operating in series with the ETF exhaust gas compressors. During the motor firing, the motor exhaust gases were used as the driving gas for the 29-in.-diam, ejector-diffuser system to maintain test cell pressure at an acceptable level.

2.3 INSTRUMENTATION

Instrumentation was provided to measure axial force, motor chamber pressure, lateral (nonaxial) force, test cell pressure, motor case and nozzle temperatures, motor rotational speed, and heat flux from the rocket plume. Table I (Appendix II) presents instrument ranges, recording methods, and measurement uncertainty for all reported parameters.

The axial force measuring system consisted of two double-bridge, strain-gage-type load cells mounted in the axial double-flexure column forward of the thrust bearing on the spacecraft centerline. The lateral (nonaxial) force measuring system consisted of two double-bridge, strain-gage-type load cells installed forward and aft between the flexure-mounted cradle and the cradle support stand normal to the rocket motor axial centerline and in the horizontal plane passing through the motor axial centerline (Fig. 2c).

Unbonded strain-gage-type transducers (0- to 1-psia) were used to measure test cell pressure. Bonded strain-gage-type transducers with ranges from 0 to 15 and 0 to 1000 psia were used to measure motor chamber pressure. Chromel®-Alumel® (CA) thermocouples were bonded to the motor case and nozzle (Fig. 3) to measure surface temperatures during and after motor burn time. Rotational speed of the motor-spacecraft assembly was determined from the output of a magnetic pickup. The heat flux from the rocket plume was measured by four radiometers mounted as shown in Fig. 4.

The output signal of each measuring device was recorded on independent instrumentation channels. Primary data were obtained from four axial thrust channels, three test cell pressure channels, and three motor chamber pressure channels. These data

were recorded as follows: Each instrument output signal was indicated in totalized digital form on a visual readout of a millivolt-to-frequency converter. A magnetic tape system, recording in frequency form, stored the signal from the converter for reduction at a later time by an electronic computer. The computer provided a tabulation of average absolute values for each 0.10-sec time increment and total integrals over the cumulative time increments.

The output signal from the magnetic rotational speed pickup was recorded in the following manner: A frequency-to-analog converter was triggered by the pulse output from the magnetic pickup and in turn supplied a square wave of constant amplitude to the electronic counter, magnetic tape, and oscillograph recorders. The scan sequence of the electronic counter was adjusted so that it directly displayed the motor spin rate in revolutions per minute.

The millivolt outputs of the lateral (nonaxial) force load cells, radiometers, and thermocouples were recorded on magnetic tape from a multi-input, analog-to-digital converter and reduced to engineering units by an electronic computer.

A recording oscillograph was used to provide an independent backup of all operating instrumentation channels except the temperature and radiation measurement systems. Selected channels of thrust and pressures were recorded on null-balance, potentiometer-type strip charts for analysis immediately after a motor firing. Visual observation of the firing was provided by a closed-circuit television monitor. High-speed, motion-picture cameras provided a permanent visual record of the firing.

2.4 CALIBRATION

The thrust system calibrator weights, thrust load cells, and pressure transducers were laboratory calibrated prior to usage in this test. After installation of the measuring devices in the test cell, the thrust load cells were again calibrated at sea-level, nonspin ambient conditions and also at simulated altitude while spinning at 46 rpm.

The pressure recording systems were calibrated by an electrical, four-step calibration, using resistances in the transducer circuits to simulate selected pressure levels. The axial thrust instrumentation systems were calibrated by applying to the thrust cradle known forces, which were produced by deadweights acting through a bell crank. The calibrator is hydraulically actuated and remotely operated from the control room. Thermocouple recording instruments were calibrated by using known millivolt levels to simulate thermocouple outputs. Calibration curves for the radiometers were supplied by the transducer manufacturer.

After the motor firing, with the test cell still at simulated altitude pressure, the recording systems were recalibrated to determine any shift.

Calibrations of the lateral (nonaxial) forces measuring system were conducted using the procedure outlined in Ref. 5.

SECTION III
PROCEDURE

The TCC TE-M-521-5 rocket motor (S/N PV32-284-1) and associated hardware arrived at AEDC on April 10, 1973. The motor was visually inspected for possible shipping damage and radiographically inspected for grain cracks, voids, or separations and found to meet criteria provided by the manufacturer.

After radiographic inspection, the motor was stored in an area temperature conditioned at 70 ± 5°F, where the motor was checked to ensure correct fit of mating hardware, the electrical resistances of the igniters were measured, and the nozzle exit diameter was obtained. The motor was leak checked after installation of the chamber pressure transducers. The entire assembly was weighed and photographed. Thermocouples had been bonded to the nozzle and motor case at the manufacturer's facilities. After the thrust adapter was secured to the motor case, the assembly was mounted on a spin table, and radial dimensions of the spacecraft flange and nozzle flange as a function of angular position relative to the centerline of the assembly were determined to facilitate alignment with the spin-rig axis during test cell installation.

After installation of the assembly in the test cell, the motor centerline was axially aligned with the spin-rig spin axis by rotating the motor assembly and measuring the deflection of the nozzle flange and the motor flange with a dial indicator and making appropriate adjustments. The instrumentation connections were made, and the motor assembly was balanced at a rotational speed of 46 rpm. Cell temperature was controlled to condition the motor assembly at 40 ± 5°F for a period in excess of 24 hr. A continuity check of all electrical systems was performed, prefire ambient calibrations were completed, the test cell pressure was reduced to the desired simulated altitude, and spinning of the unit was started. After spinning had stabilized at 46 rpm, a complete set of altitude calibrations was taken.

The final operation prior to firing the motor was to adjust the firing circuit resistance to provide the desired current to the igniter squibs. The entire instrumentation measuring-recording complex was activated, and the motor was fired while spinning (under power) at 46 rpm.

Spinning the motor was continued for approximately 60 min after burnout, during which time motor temperatures were recorded and postfire calibrations were accomplished. The unit was decelerated slowly until rotation had stopped, and another set of calibrations was taken. The test cell pressure was then returned to ambient conditions, and the motor assembly was inspected, photographed, and removed to the storage area. Postfire inspections at the storage area consisted of measuring the throat and exit diameters of the nozzle, weighing the motor, and photographically recording the postfire condition of the motor.

SECTION IV
RESULTS AND DISCUSSION

One Thiokol Chemical Corporation TE-M-521-5 solid-propellant rocket motor (S/N PV32-284-1) was successfully fired at an average altitude of 103,000 ft. The motor was prefire vibration conditioned and temperature conditioned at 40 ± 5°F for a period in excess of 24 hr prior to firing with the motor assembly spinning about the motor longitudinal axis at 46 rpm. The general objective of this quality assurance program was to verify compliance of motor performance with the manufacturer's specifications (Ref. 4). Specific primary objectives were to determine vacuum ballistic performance, altitude ignition characteristics, motor structural integrity, and motor temperature-time histories during and after motor operation. Secondary objectives were to measure the motor lateral (nonaxial) thrust component during motor operation and to measure radiation heat flux in the vicinity of the nozzle exit plane. The resulting data are presented in both tabular and graphical form.

Motor performance based on action time (t_a) and total burn time (t_{is}) is summarized and compared with results from previous altitude firings of the TE-M-521-5 in Table II. Motor physical dimensions are compared with those of the previous motors in Table III. Altitude ignition characteristics, rocket exhaust plume radiation heat flux, and temperature-time histories of the motor case and nozzle are presented and discussed. When multiple channels of equal accuracy instrumentation were used to obtain values of a single parameter, the average values were used to calculate the data presented.

4.1 ALTITUDE IGNITION CHARACTERISTICS

The motor was ignited at a pressure altitude of 117,000 ft. The average simulated altitude during motor action time (t_a) was 103,000 ft. Variations of thrust and chamber pressure during motor ignition are presented in Fig. 5.

Ignition time (t_i) was 0.185 sec and was within the manufacturer's specifications of not less than 0.025 sec or greater than 0.250 sec for a temperature range of from 0 to 110°F. Ignition lag time (t_ℓ) was 0.006 sec, utilizing only one pyrogen igniter. The ignition lag times of the motors previously tested at the AEDC, which were temperature conditioned at 40°F, were 0.002 sec (Ref. 2), utilizing two pyrogen igniters, and 0.006 sec (Ref. 3), utilizing two pyrogen igniters. Ignition lag times of all TE-M-521-5 motors tested at the AEDC were within the manufacturer's estimated value of 0.006 ± 0.005 sec.

4.2 ALTITUDE BALLISTIC PERFORMANCE

Since the nozzle does not operate fully expanded at the low chamber pressures encountered during tailoff, the measured total impulse data during this period cannot be corrected to vacuum conditions by adding the product of cell pressure integral and nozzle exit area. Therefore, total burn time and action time were segmented, and the method

used to determine vacuum impulse is illustrated in Fig. 6. The time of exhaust nozzle flow breakdown (t_{bd}) was considered to have occurred simultaneously with the exhaust diffuser flow breakdown (as indicated by a rapid increase in cell pressure during tailoff). The flow velocity at the nozzle throat was considered sonic until the time (t_{is}) at which the ratio of chamber-to-cell pressure had decreased to a value of 1.3. The time interval (t_1 to t_2) is a one-second interval of motor operation just prior to decrease in chamber pressure (Fig. 6).

Performance characteristics of the motor reported herein and the two previously fired TE-M-521-5 motors (Refs. 2 and 3) are presented in Table II and Fig. 7. Action time (t_a) for motor S/N PV32-284-1 was 20.60 sec, compared with 21.26 sec and 20.68 sec for the motors of Ref. 2 and 3, respectively, which were fired at the same spin rate (46 rpm) and temperature (40°F) as the motor reported herein. The total burn time (t_{is}) for motor S/N PV32-284-1 was 34.50 sec. Vacuum total impulse was 71,637 lbf-sec for motor S/N PV32-284-1 and agreed within 0.25 percent of the vacuum impulse of the Ref. 2 and 3 motors. All three motors were within the manufacturer's specification of vacuum total impulse of 71,350 ± 350 lbf-sec, 3σ deviation. Vacuum specific impulse of motor S/N PV32-284-1 (based on t_{is} and the manufacturer's stated propellant weight) was 289.69 lbf-sec/lbm. Vacuum specific impulse based on the expended mass, as determined by pre- and postfire motor weight measurements taken at the AEDC, was 286.38 lbf-sec/lbm for the motor reported herein, compared with 286.83 lbf-sec/lbm for the Ref. 2 motor and 288.76 lbf-sec/lbm for the Ref. 3 motor.

4.3 STRUCTURAL INTEGRITY AND MOTOR TEMPERATURE-TIME HISTORY

External postfire examination of the motor case and nozzle assembly did not reveal any evidence of thermal damage (Fig. 8). The pinned nozzle throat section was securely in place after the test. Nozzle throat measurements indicated a throat area increase of 11.7 percent of the prefire area. The nozzle exit area had decreased approximately 0.78 percent from the prefire area.

Motor case and nozzle temperature variations with time are presented in Fig. 9. The maximum indicated case temperature (490°F) occurred approximately 300 sec after motor ignition, as indicated by the thermocouple (TC-7) located on the motor case near the nozzle closure (Fig. 9b) and was within the maximum manufacturer's limit of 600°F. The maximum case temperature recorded during the previous -5 motor test was 525°F, 600 sec after motor ignition (Ref. 2) and 590°F, 300 sec after motor ignition (Ref. 3). The maximum indicated nozzle temperature (550°F) occurred 500 sec after motor ignition, as indicated by the thermocouples (TN-14 and TN-31) located near the nozzle throat (Fig. 9k); the previous maximum nozzle temperature was 705°F, 245 sec after motor ignition (Ref. 2 motor) and 560°F, 150 sec after motor ignition (Ref. 3 motor). The Ref. 2 motor was enclosed in a flightweight thermal insulation blanket.

The maximum motor case temperature in the region where the relief boot was removed (Fig. 1c) was about 470°F (TC-30, Fig. 9h) and occurred about 500 sec after motor ignition.

Comparable temperature measurements were not made in this region for the tests reported in Refs. 2 and 3; however comparable maximum temperature measurements adjacent to this region (TC-10 and TC-23) (375 to 430°F) were of approximately the same magnitude as those reported in Refs. 2 and 3.

4.4 EXHAUST PLUME RADIATION

Four narrow-angle radiometers were used to obtain rocket exhaust plume radiation heat flux data. The instruments were positioned around the nozzle assembly as shown in Fig. 4.

The variation of radiation heat flux with time is presented in Fig. 10. The maximum radiation heat flux (prior to motor burnout and diffuser breakdown) was 18 Btu/ft^2-sec (Fig. 10d, R-6) and occurred 19 sec after ignition. The maximum measured radiation on the motor reported herein and on the Ref. 3 motor was 3 Btu/ft^2-sec higher than the maximum measured during the Ref. 2 motor. Measured radiation heat flux increased throughout the firing.

4.5 LATERAL (NONAXIAL) THRUST VECTOR MEASUREMENT

An additional objective for this test was to measure the lateral (nonaxial) component of motor thrust. The recorded lateral thrust data were corrected for installation and/or electronic effects.

The maximum magnitude of lateral thrust recorded during the near steady-state portion of motor operation was 3.9 lbf and occurred at approximately 17 sec after motor ignition (Fig. 11). The corresponding angular position of the lateral thrust vector (measured clockwise looking upstream) was 90 deg.

SECTION V
SUMMARY OF RESULTS

One Thiokol Chemical Corporation TE-M-521-5 solid-propellant rocket motor was successfully fired at an average pressure altitude of about 103,000 ft, while spinning at 46 rpm about the motor axis. The motor was prefire vibration conditioned, and temperature conditioned in a controlled environment of 40 ± 5°F for a period in excess of 24 hr prior to firing. Results are summarized as follows:

1. Ignition time (t_i), the time interval from application of ignition voltage to attainment of 90 percent of peak thrust during the ignition transient, was 0.185 sec and met the manufacturer's specifications of from 0.025 to 0.250 sec.

2. Ignition lag time (t_ℓ), the time interval from the time at which ignition voltage was applied to the igniter circuit to the first perceptible rise in chamber pressure, was 0.006 sec. Only one of the two pyrogen igniters was utilized in the ignition sequence.

3. Action time (t_a), the time interval between 10 percent of maximum chamber pressure during ignition and 10 percent of maximum chamber pressure during tailoff, was 20.60 sec.

4. Total burn time (t_{is}), the time interval from the application of ignition voltage to the time at which the ratio of chamber-to-cell pressure had decreased to 1.3 at tailoff, was 34.50 sec.

5. Vacuum total impulse, based on t_{is}, was 71,637 lbf-sec, and was within the manufacturer's specification of 71,350 ± 350 lbf-sec. Vacuum specific impulse, based on t_{is} and expended mass, was 286.38 lbf-sec/lbm.

6. The nozzle throat area increased approximately 11.7 percent from the prefire area during the firing. The nozzle exit area decreased nominally 0.78 percent.

7. The maximum motor case temperature was 490°F and occurred approximately 300 sec after motor ignition. The maximum nozzle temperature was 550°F and occurred approximately 500 sec after ignition.

8. The maximum magnitude of lateral (nonaxial) thrust measured during near steady-state portion of motor operation was 3.9 lbf and occurred at approximately 17 sec after first indication of motor ignition.

9. The maximum radiation heat flux was 18 Btu/ft^2 sec at the exit plane 19 sec after ignition and was within the range measured during previous tests. Measured radiation heat flux increased throughout the firing.

10. The modification to the aft pressure relief boot appeared to have no effect on motor ballistic performance or motor structural integrity.

REFERENCES

1. Belvins, Jay. "IMP Kick Motor Test Plan, Test 5205-191." Thiokol Chemical Corporation, Elkton, Maryland, April 1973.

2. Cimino, A. A. "Evaluation of the Thiokol TE-M-521-5 Apogee Kick Motor Tested in the Spin Mode at Simulated Altitude Conditions." AEDC-TR-72-85 (AD747081), August 1972.

3. Cimino, A. A. "Design Assurance Test of the Thiokol TE-M-521-5 Apogee Kick Motor Tested in the Spin Mode at Simulated Altitude Conditions." AEDC-TR-73-15 (AD756838), March 1973.

4. NAS 7-801 Specifications. "TE-M-521-5 Apogee Motor." GSFC TCN 470-18475, April 13, 1971.

APPENDIXES
I. ILLUSTRATIONS
II. TABLES

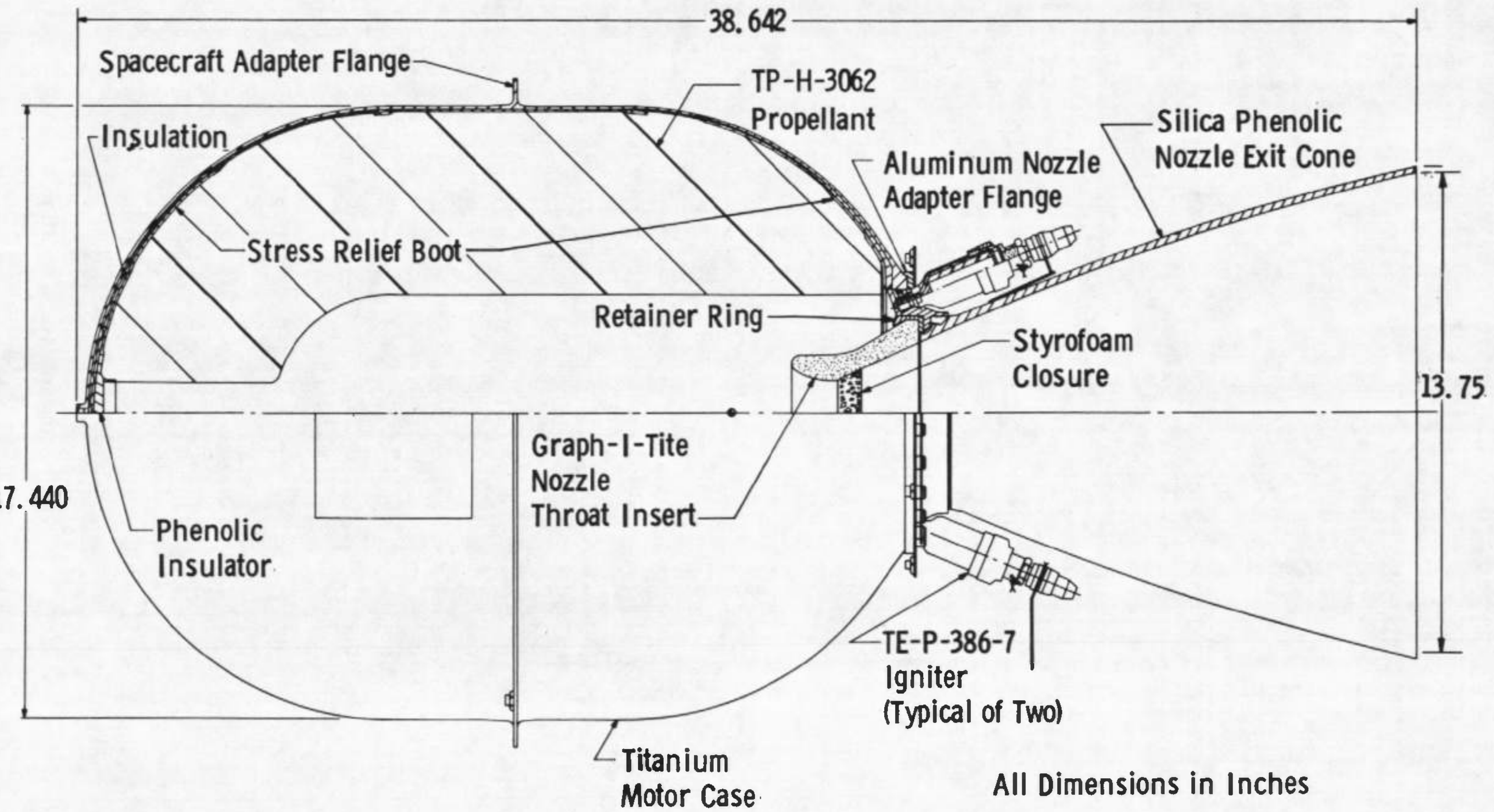

a. Schematic

Fig. 1 Thiokol Chemical Corporation TE-M-521-5 Rocket Motor

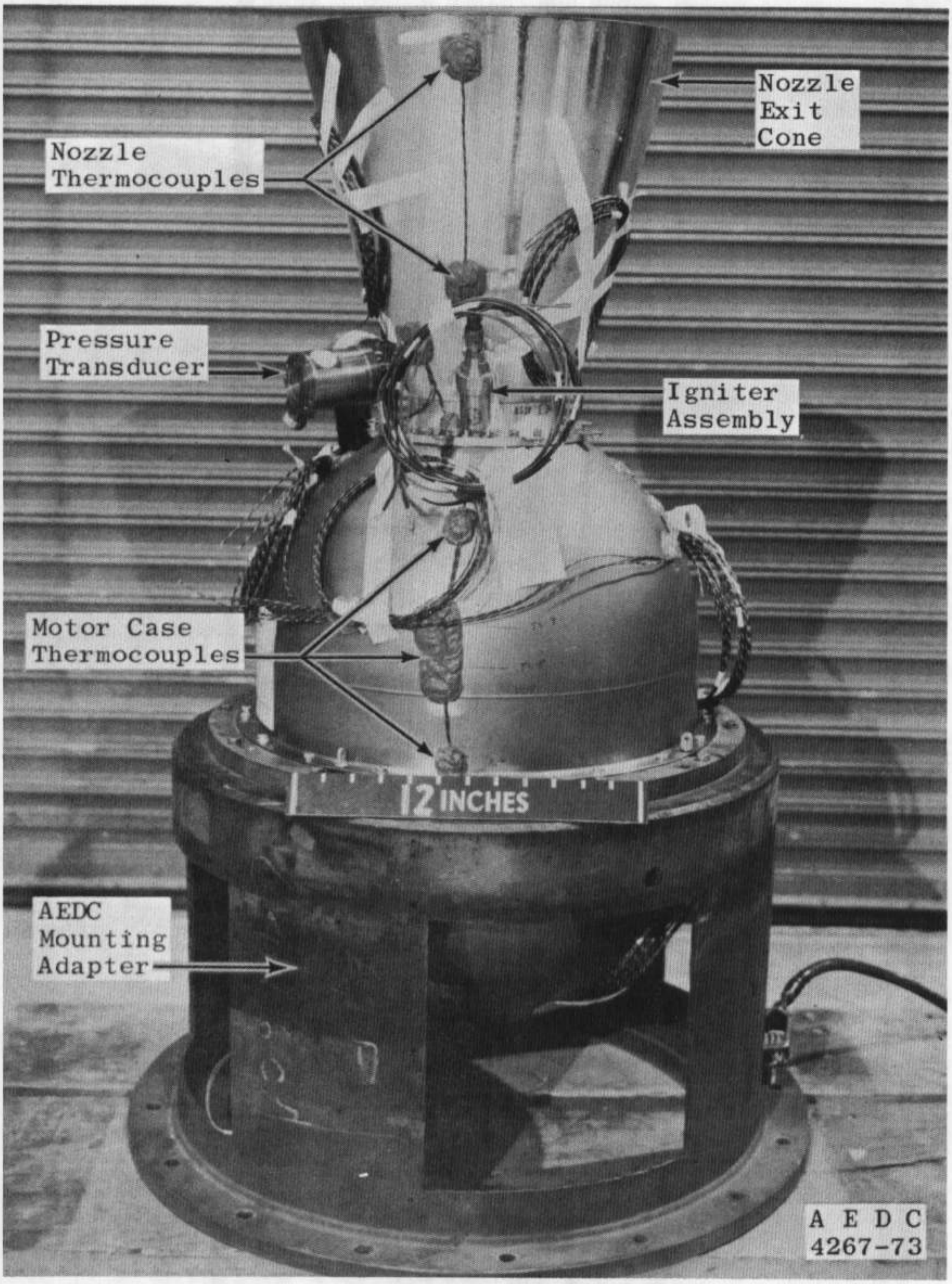

b. Photograph (Less Igniters)
Fig. 1 Continued

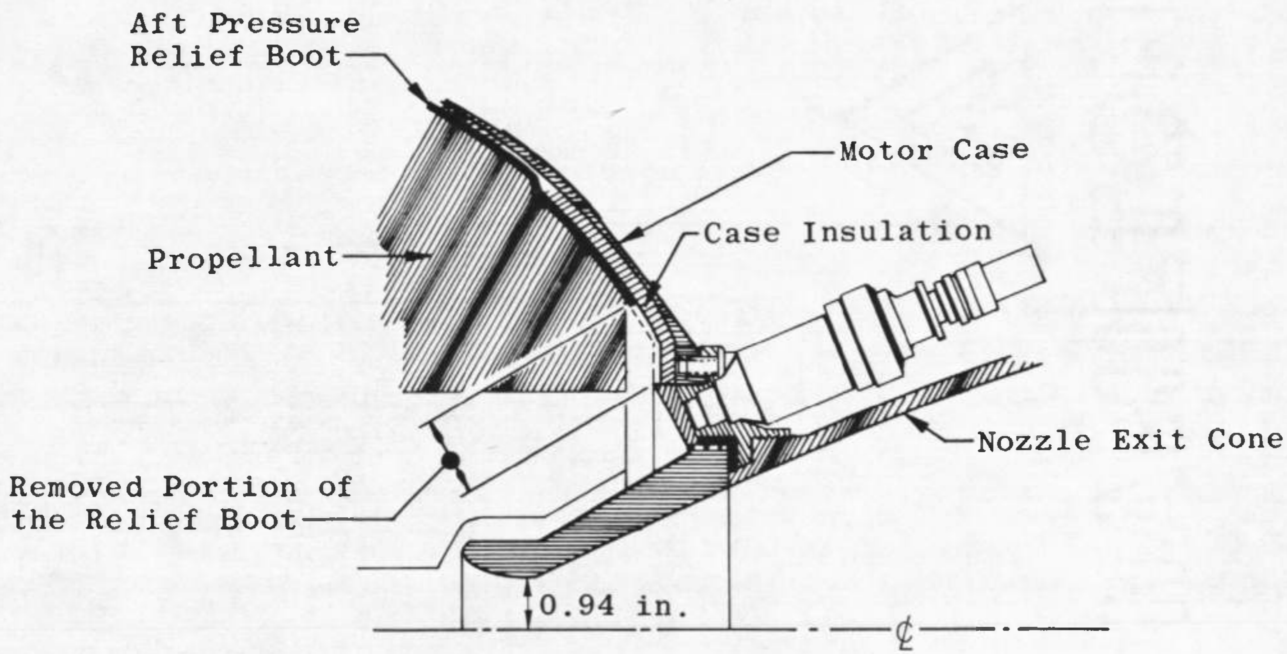

c. Schematic of Relief Boot Removal
Fig. 1 Concluded

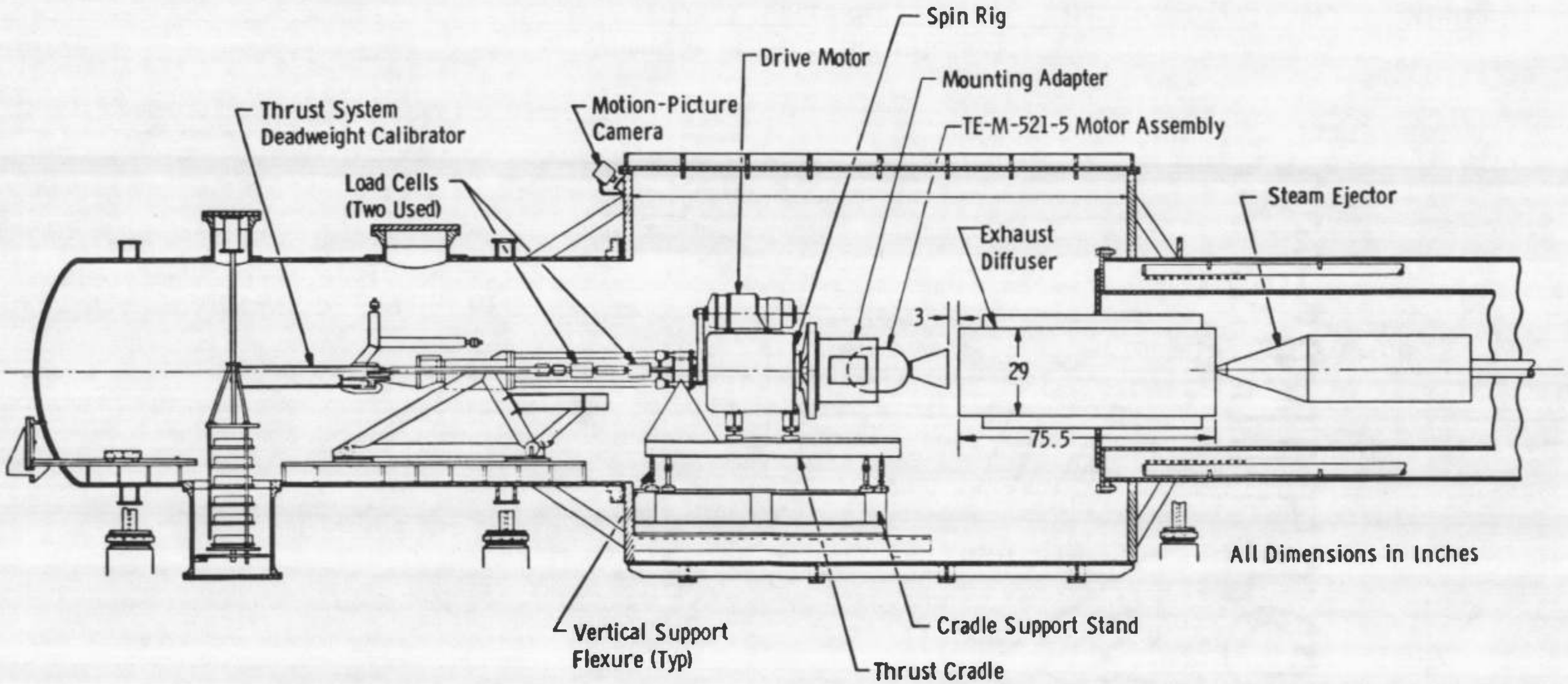

a. Schematic

Fig. 2 Installation of the Thiokol TE-M-521-5 Motor in Propulsion Development Test Cell (T-3)

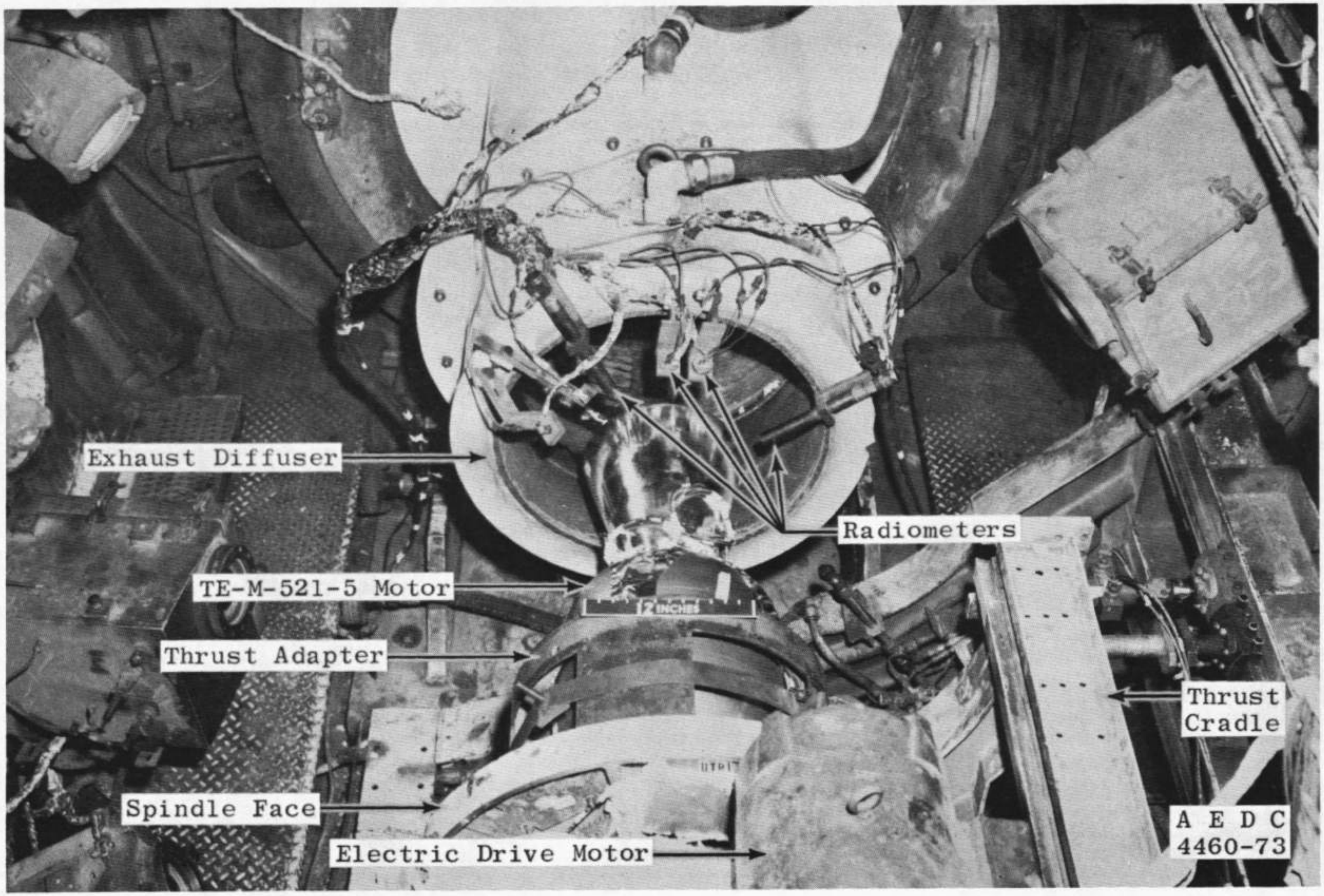

b. Photograph
Fig. 2 Continued

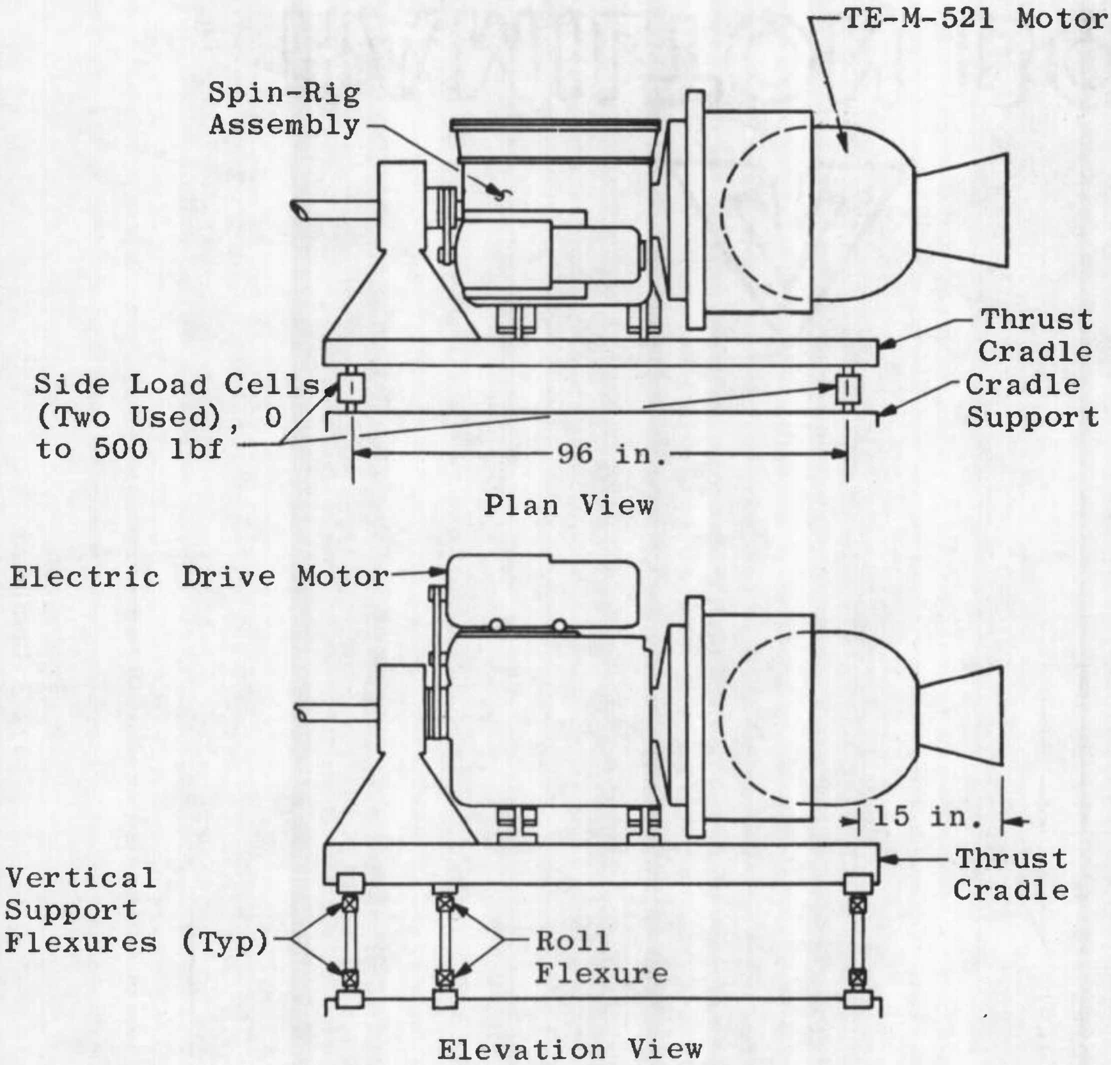

c. Details of Nonaxial Force Measuring System
Fig. 2 Concluded

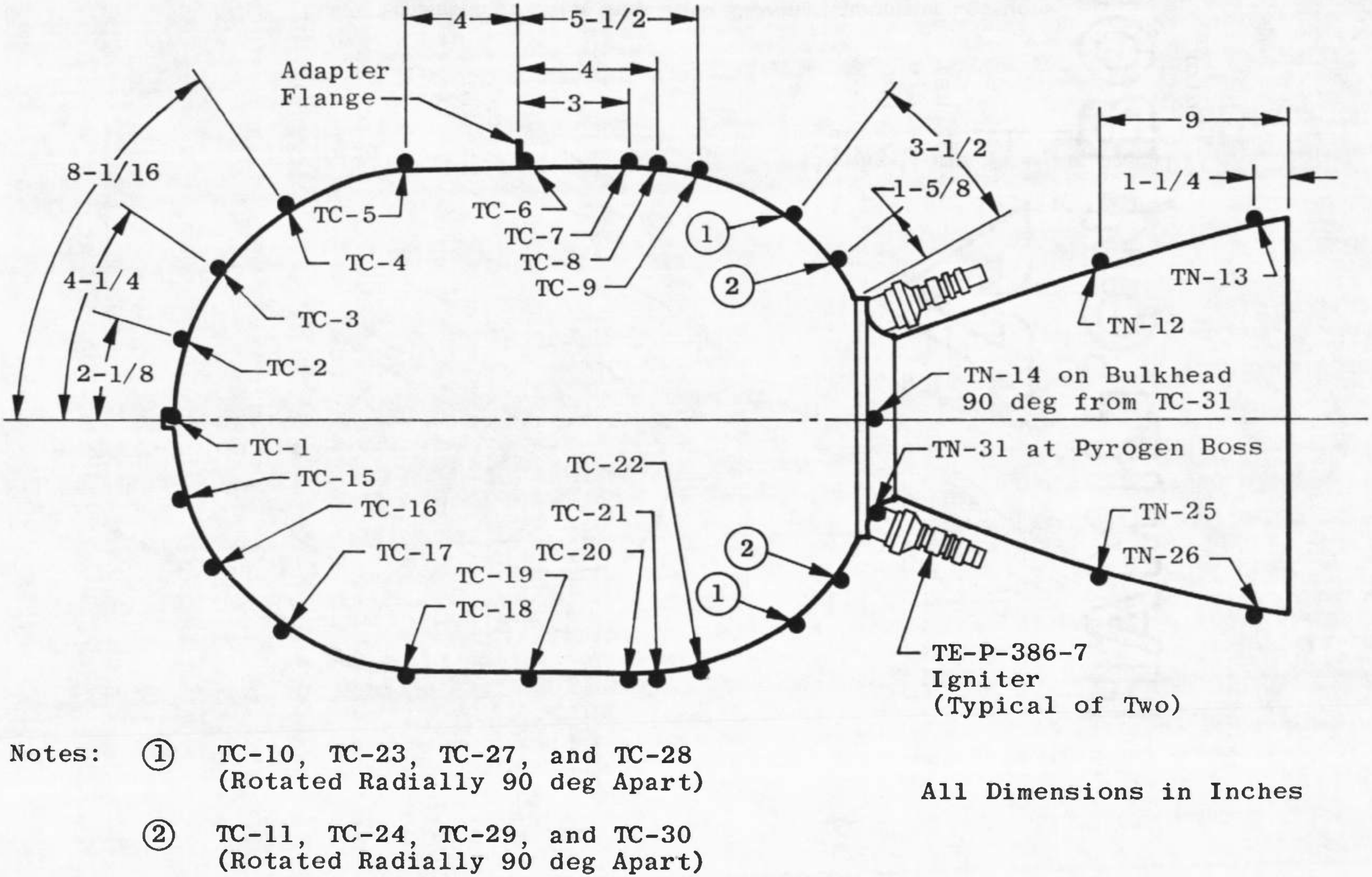

Fig. 3 Schematic of Motor Showing Thermocouple Locations

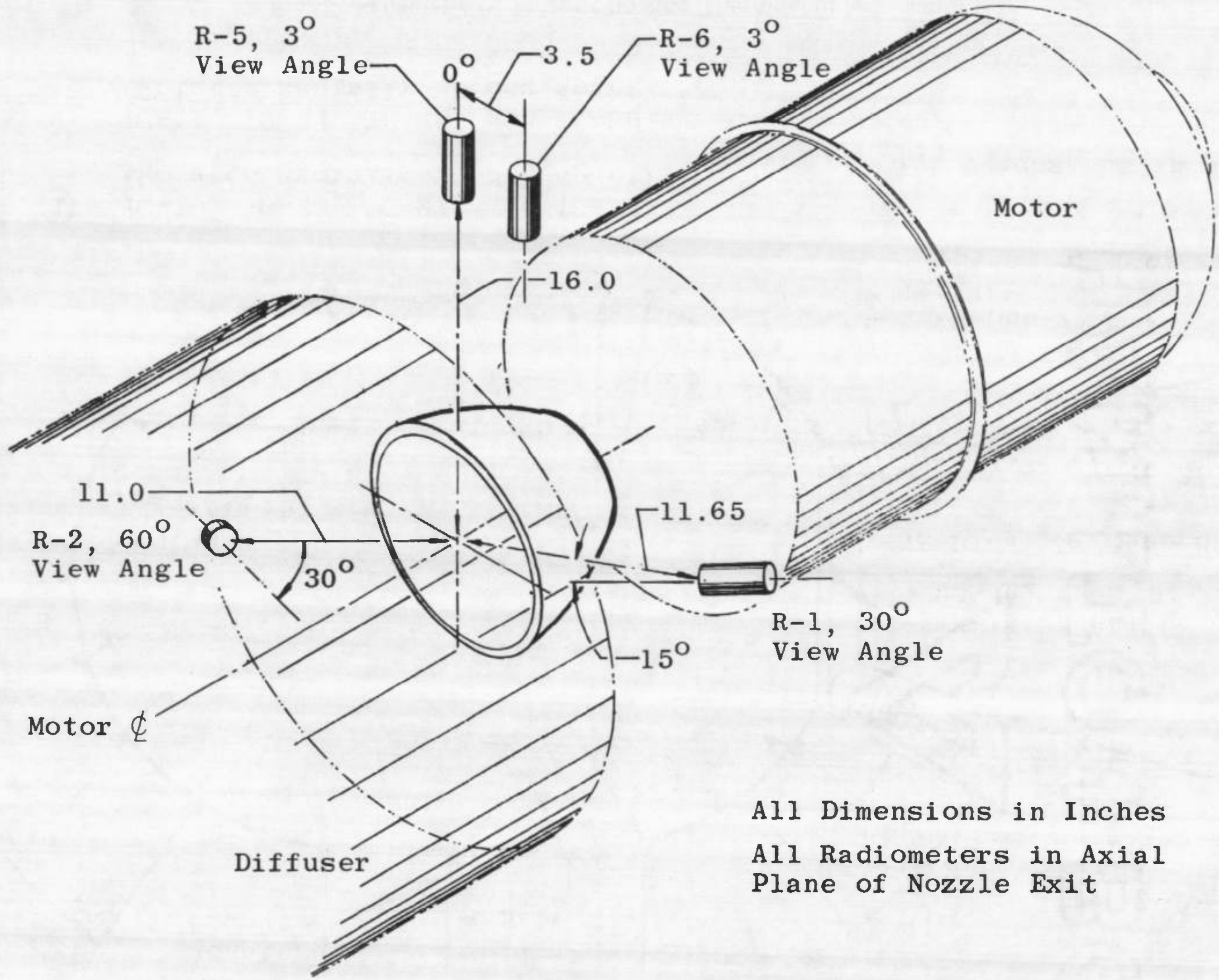

Fig. 4 Schematic of Motor Installation Showing Radiometer Locations

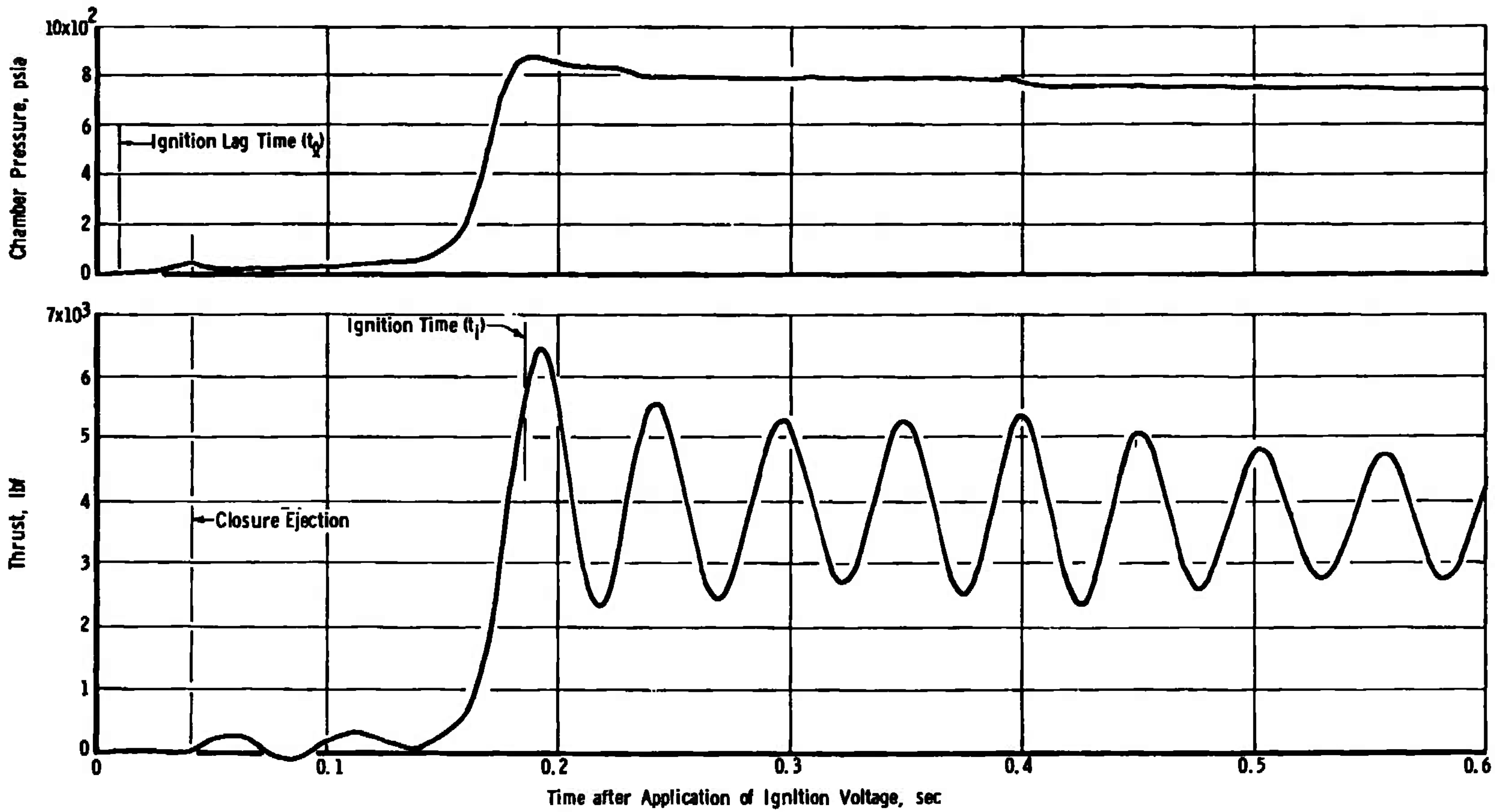

Fig. 5 Variation of Thrust and Chamber Pressure during the Ignition Event

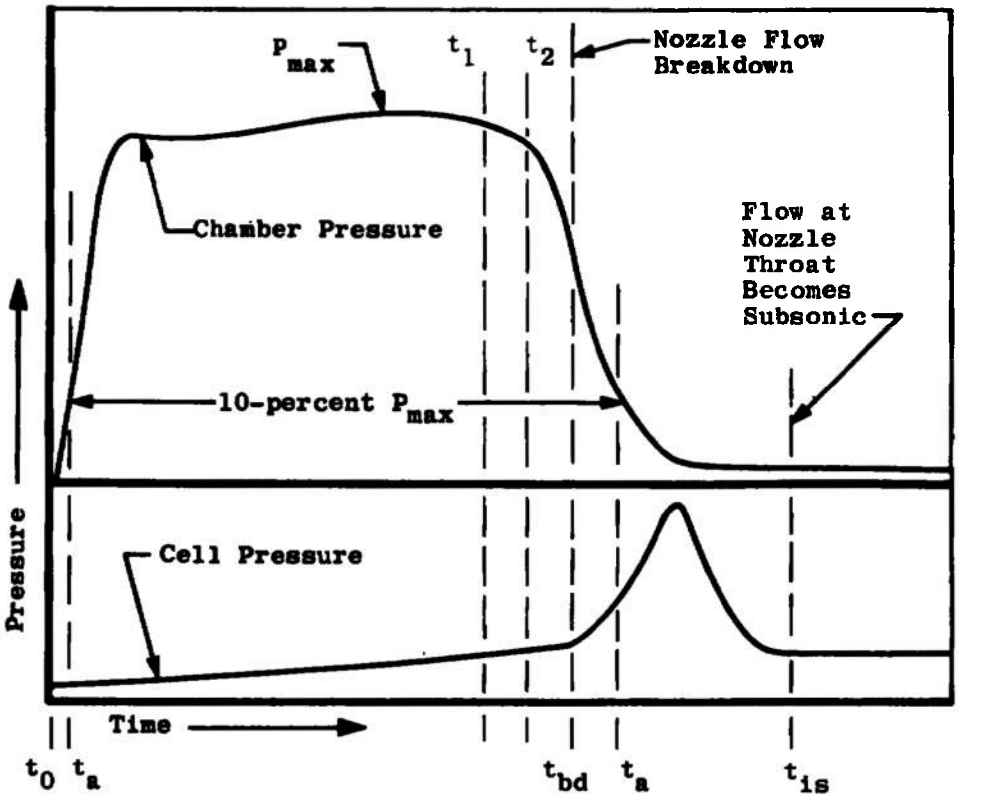

$$I_{vac_{total}} = \int_{t_0}^{t_{bd}} F\,dt + A_{ex(avg)} \int_{t_0}^{t_{bd}} P_{cell}\,dt + \bar{c}_f\,A_{th(post)} \int_{t_{bd}}^{t_{is}} P_{ch}\,dt$$

$$I_{vac_{action}} = \int_{t_{a_{ignition}}}^{t_{bd}} F\,dt + A_{ex(avg)} \int_{t_{a_{ignition}}}^{t_{bd}} P_{cell}\,dt + \bar{c}_f\,A_{th(post)} \int_{t_{bd}}^{t_{a_{tailoff}}} P_{ch}\,dt$$

where: $$\bar{c}_f = \frac{\int_{t_1}^{t_2} F\,dt + A_{ex_{post}} \int_{t_1}^{t_2} P_{cell}\,dt}{A_{t_{post}} \int_{t_1}^{t_2} P_{ch}\,dt}$$

established from data during the time interval from 17.9 (t_1) to 18.9 (t_2) sec after first indication of chamber pressure.

Fig. 6 Definition of Vacuum Total and Action Impulse

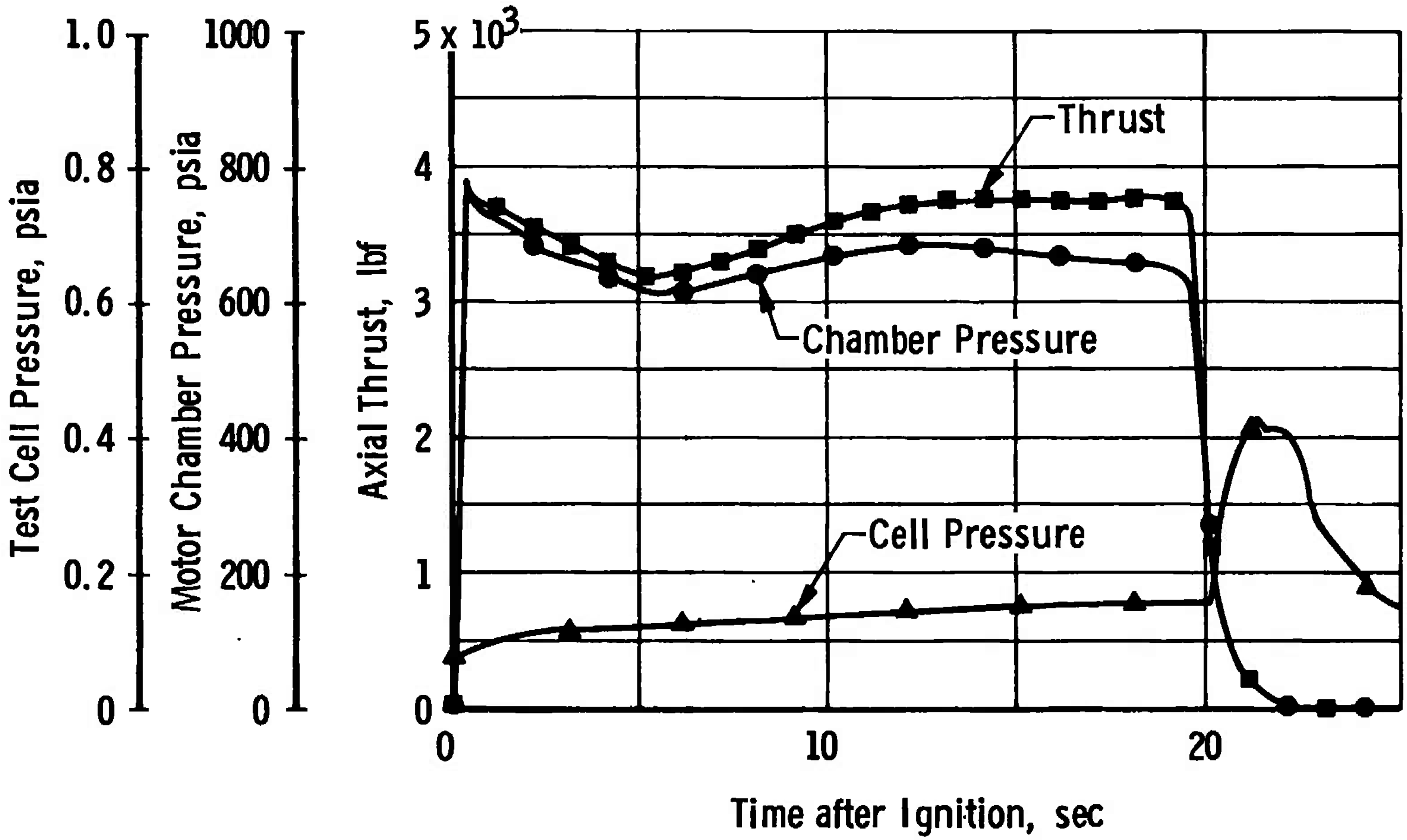

Fig. 7 Variation of Thrust, Chamber Pressure, and Test Cell Pressure during Firing

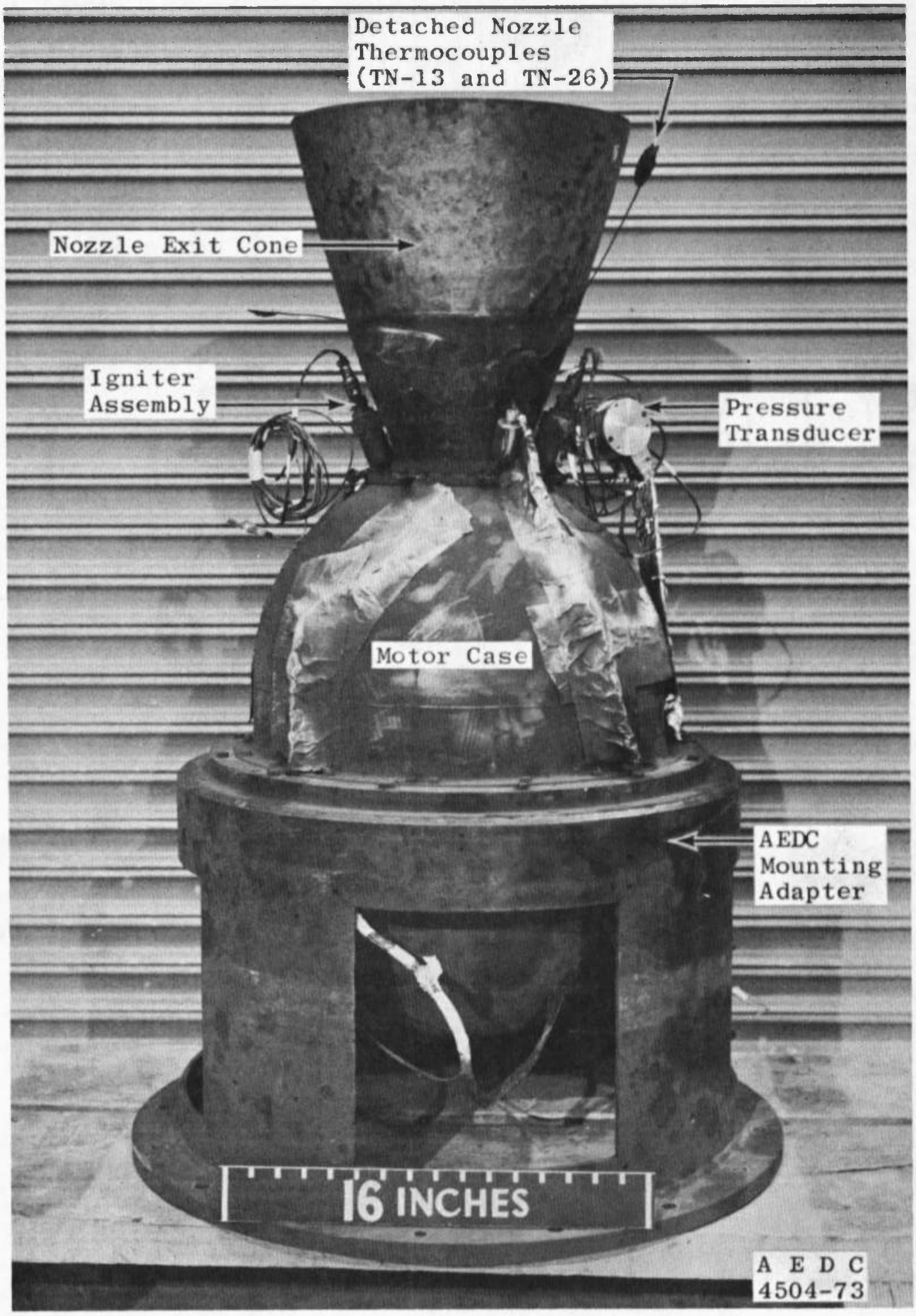

a. Motor Case and Nozzle
Fig. 8 Postfire Photographs of Motor Assembly

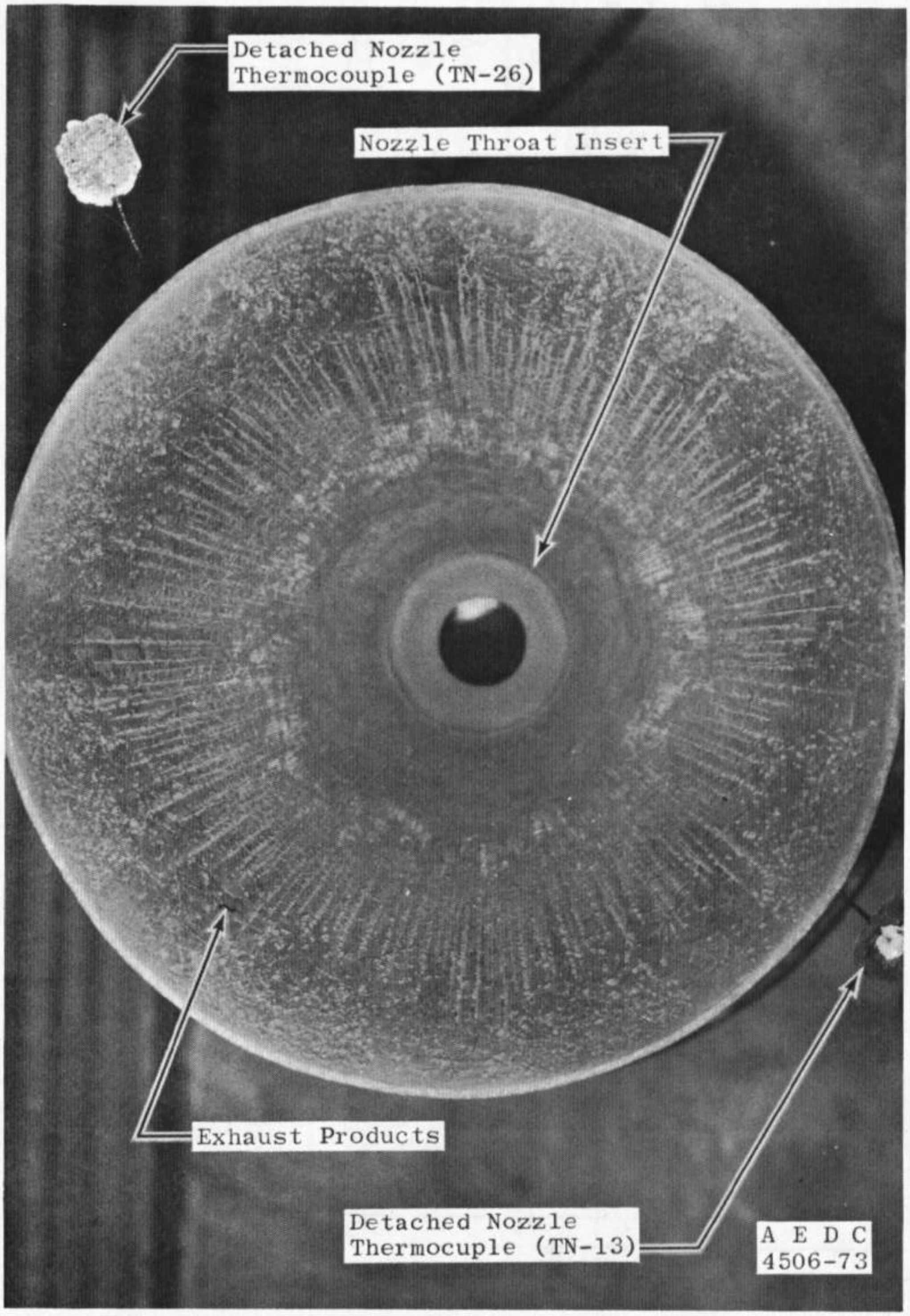

b. Nozzle
Fig. 8 Concluded

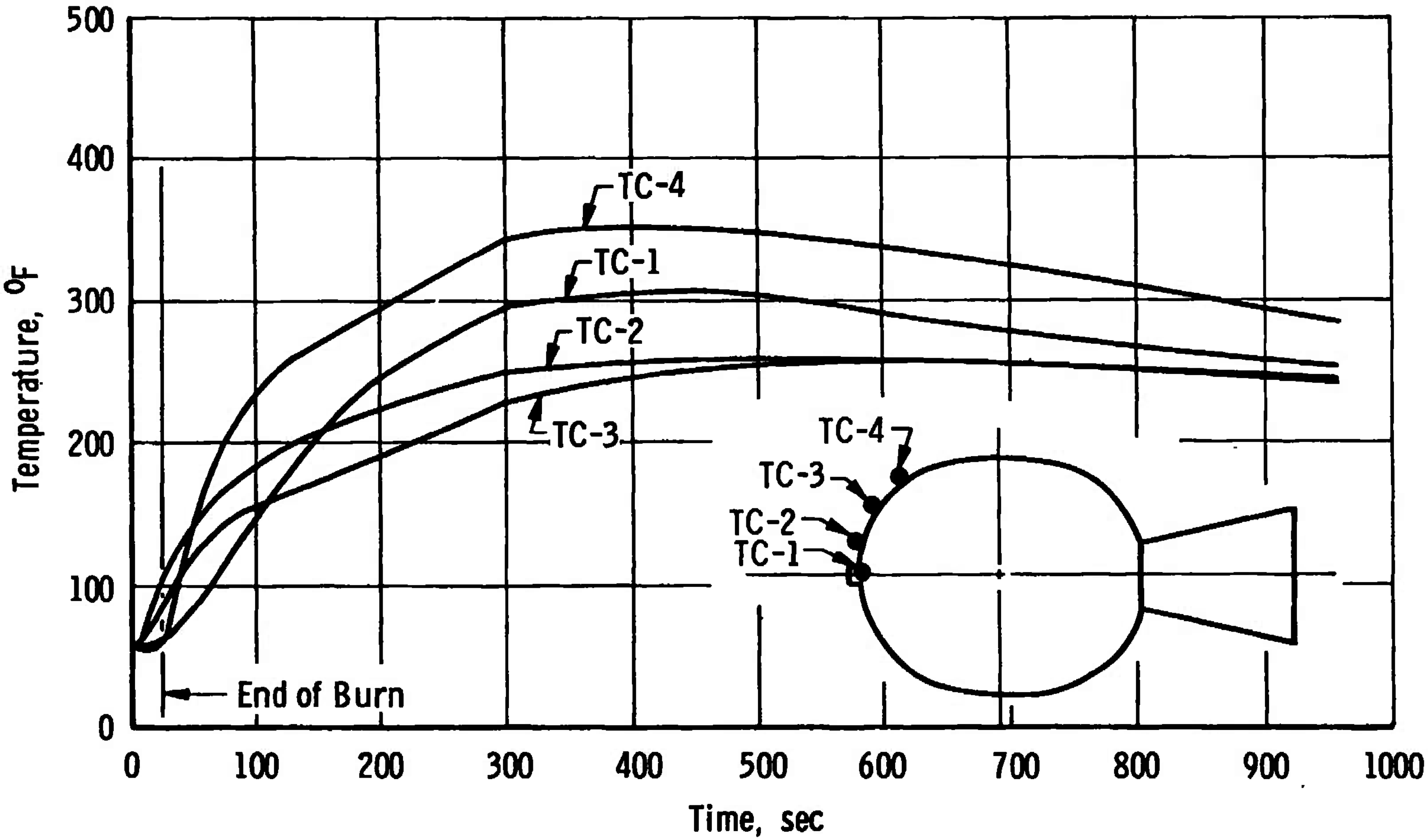

a. Motor Case; TC-1, TC-2, TC-3, and TC-4
Fig. 9 Motor Temperature Variation with Time

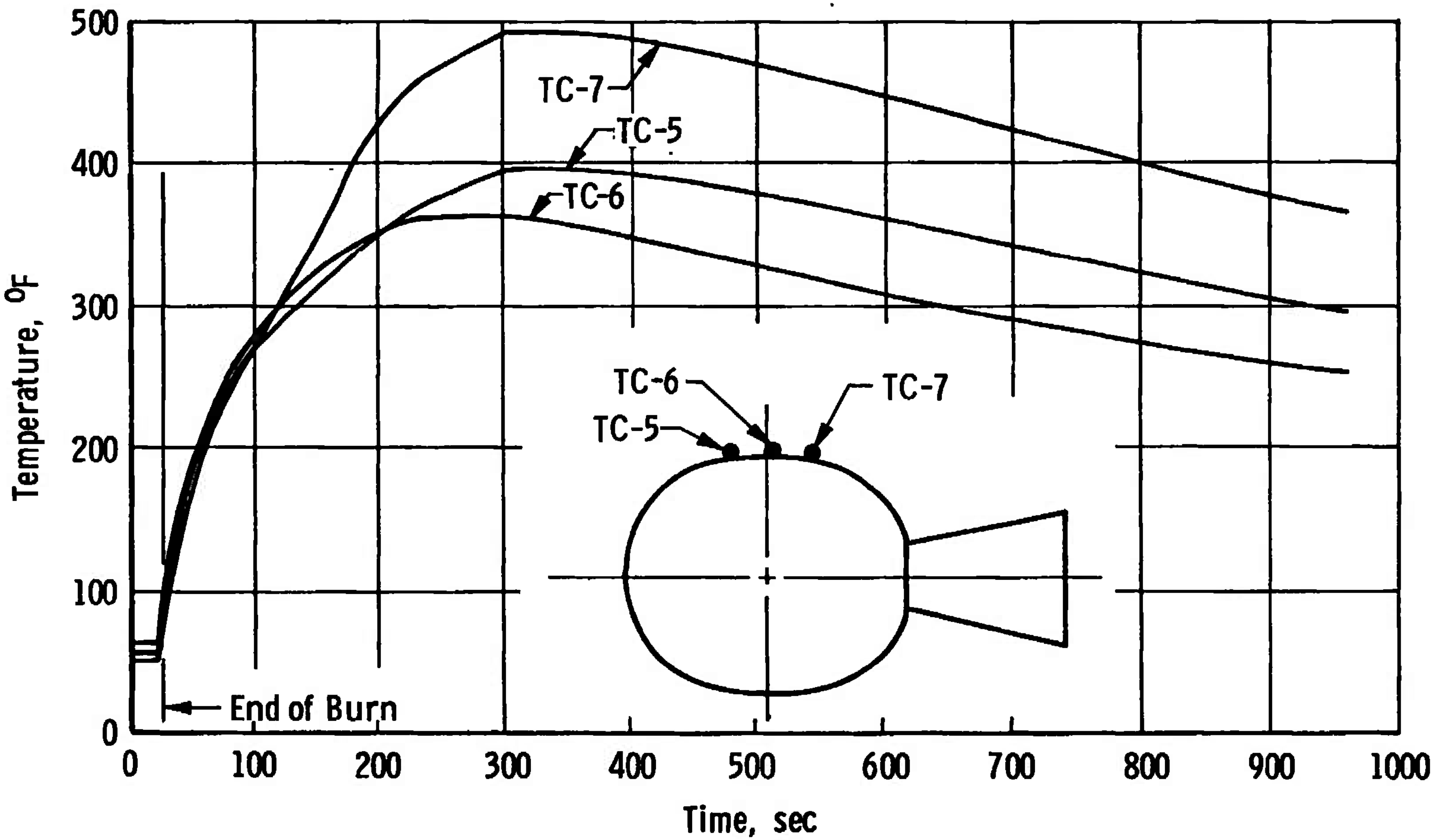

b. Motor Case; TC-5, TC-6, and TC-7
Fig. 9 Continued

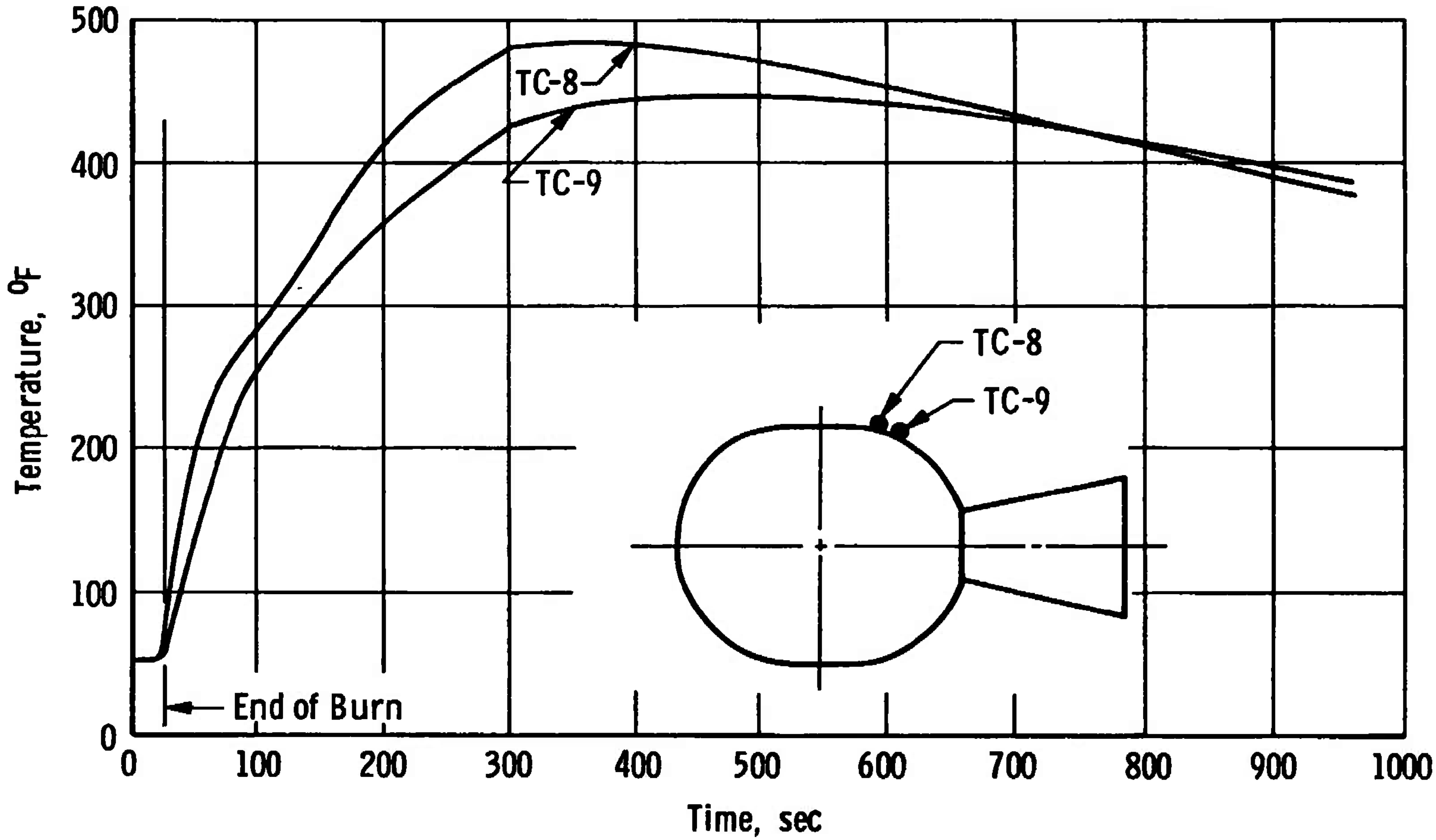

c. Motor Case; TC-8 and TC-9
Fig. 9 Continued

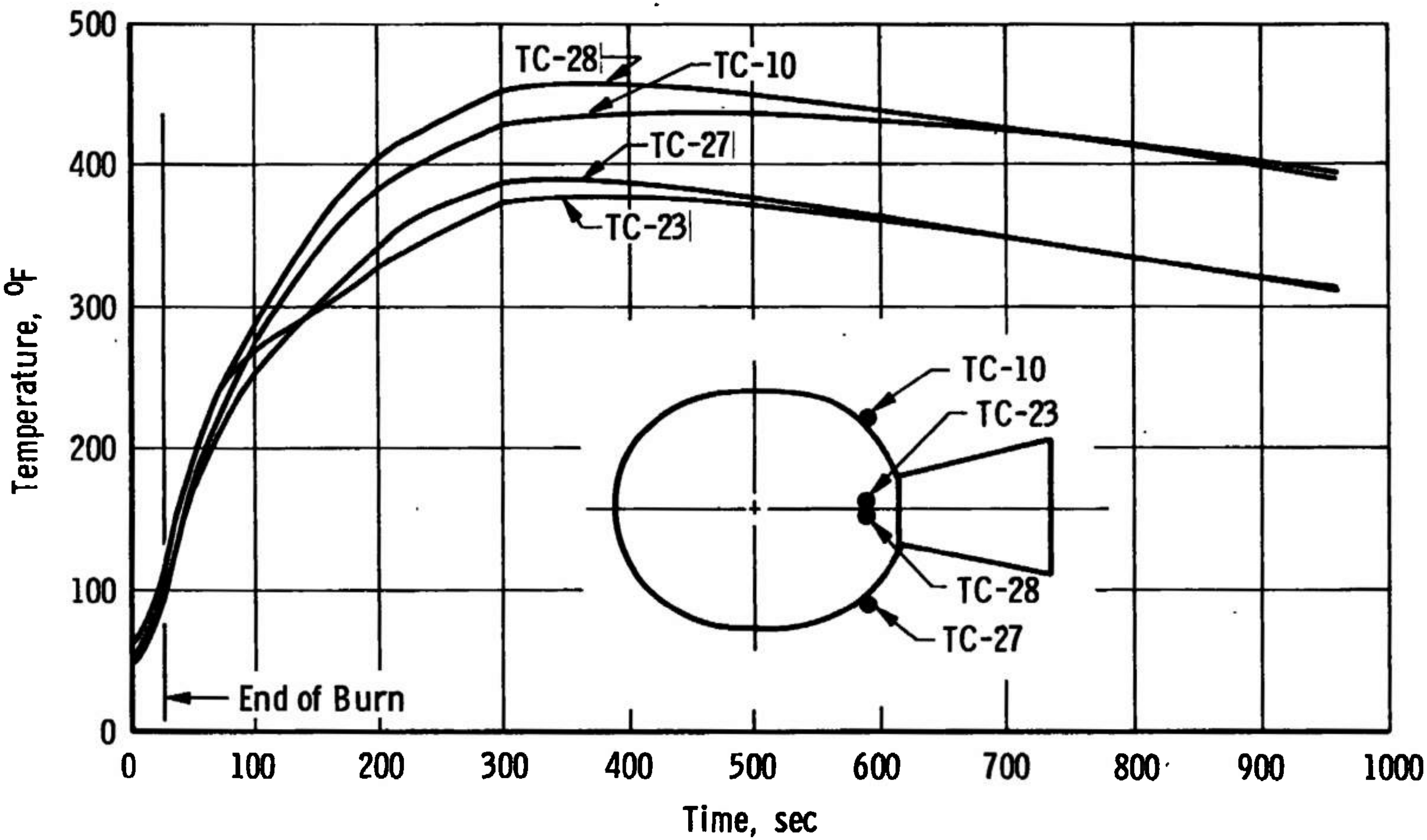

d. Motor Case; TC-10, TC-23, TC-27, and TC-28
Fig. 9 Continued

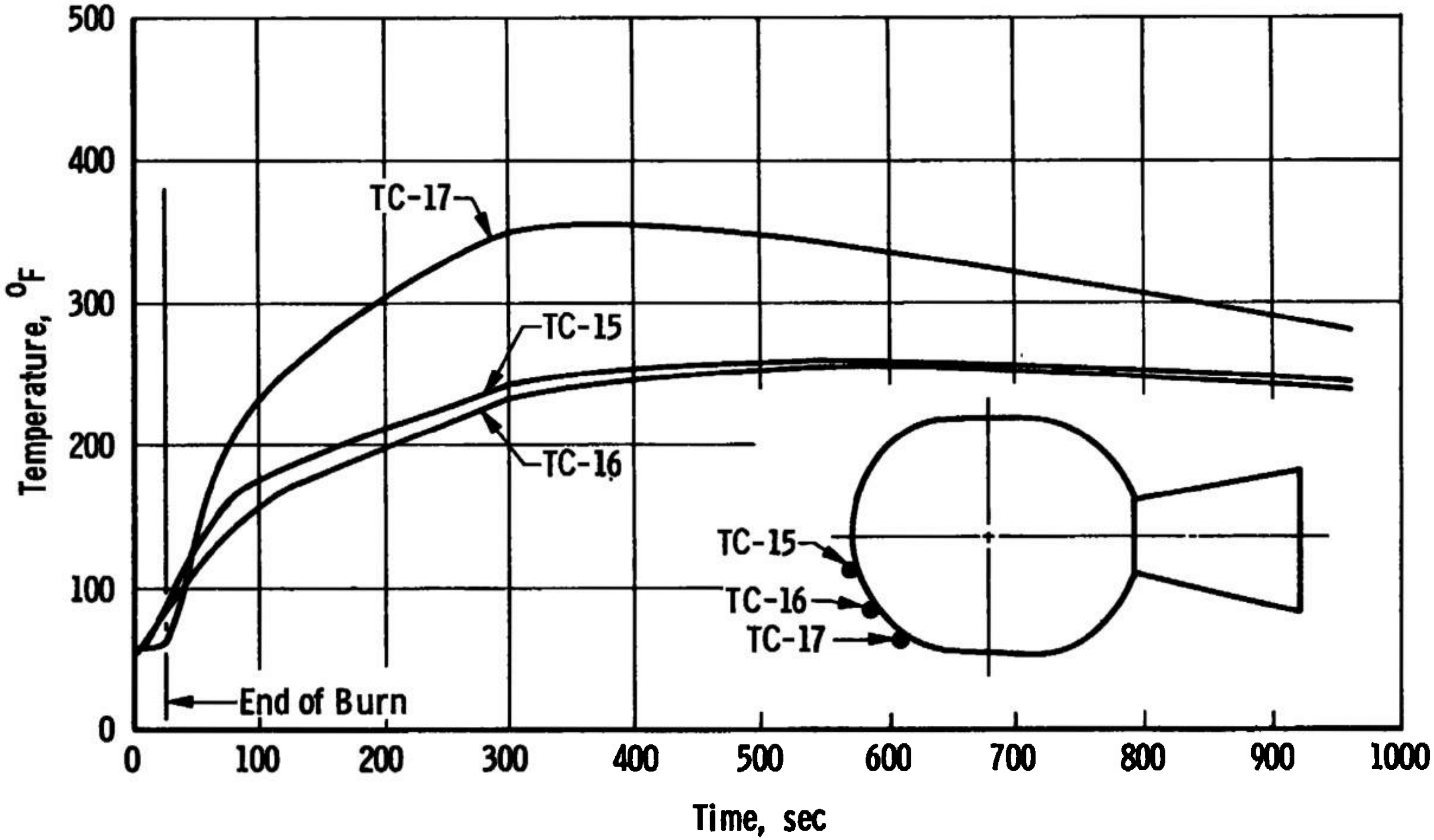

e. Motor Case; TC-15, TC-16, and TC-17
Fig. 9 Continued

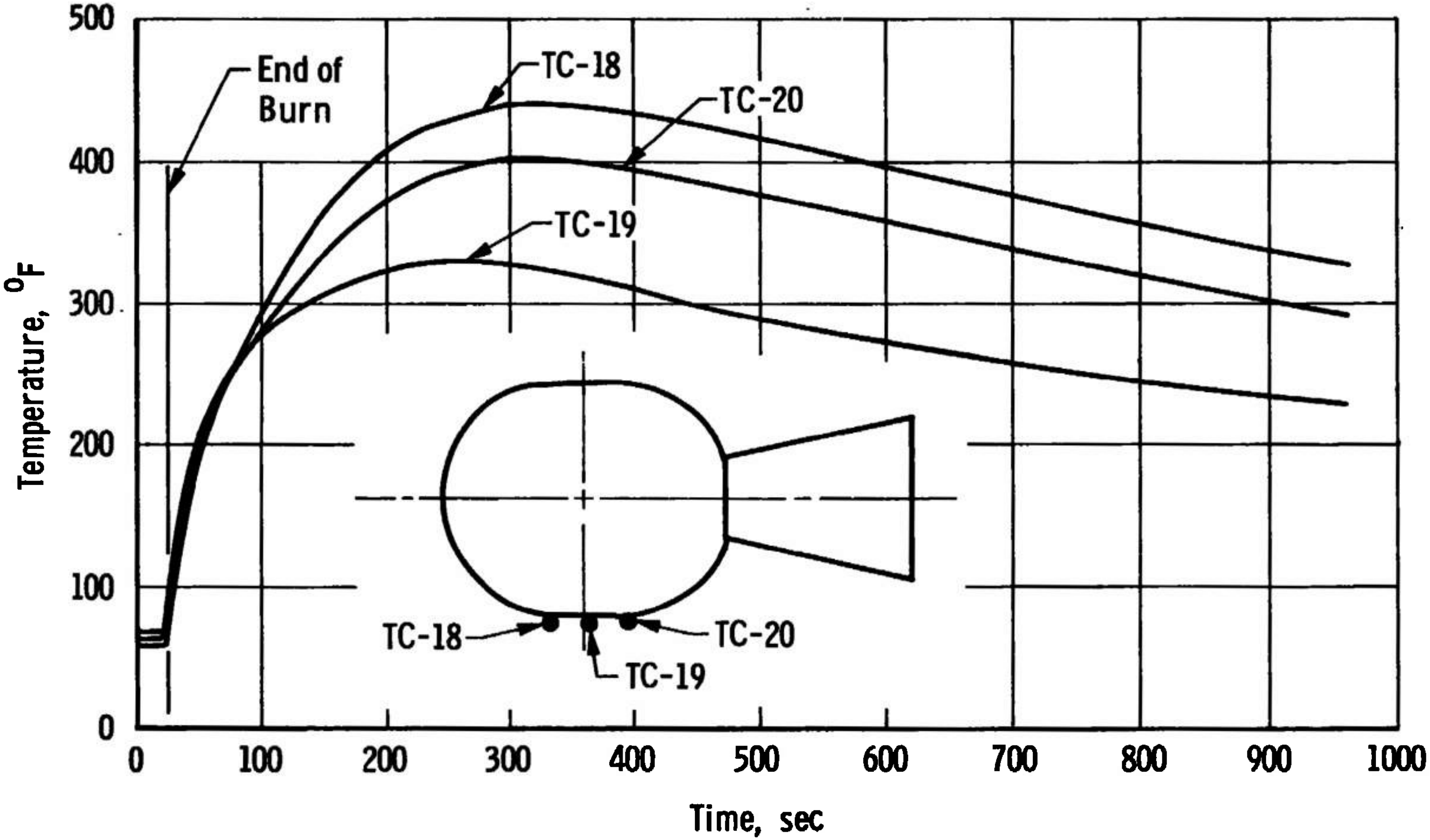

f. Motor Case; TC-18, TC-19, and TC-20
Fig. 9 Continued

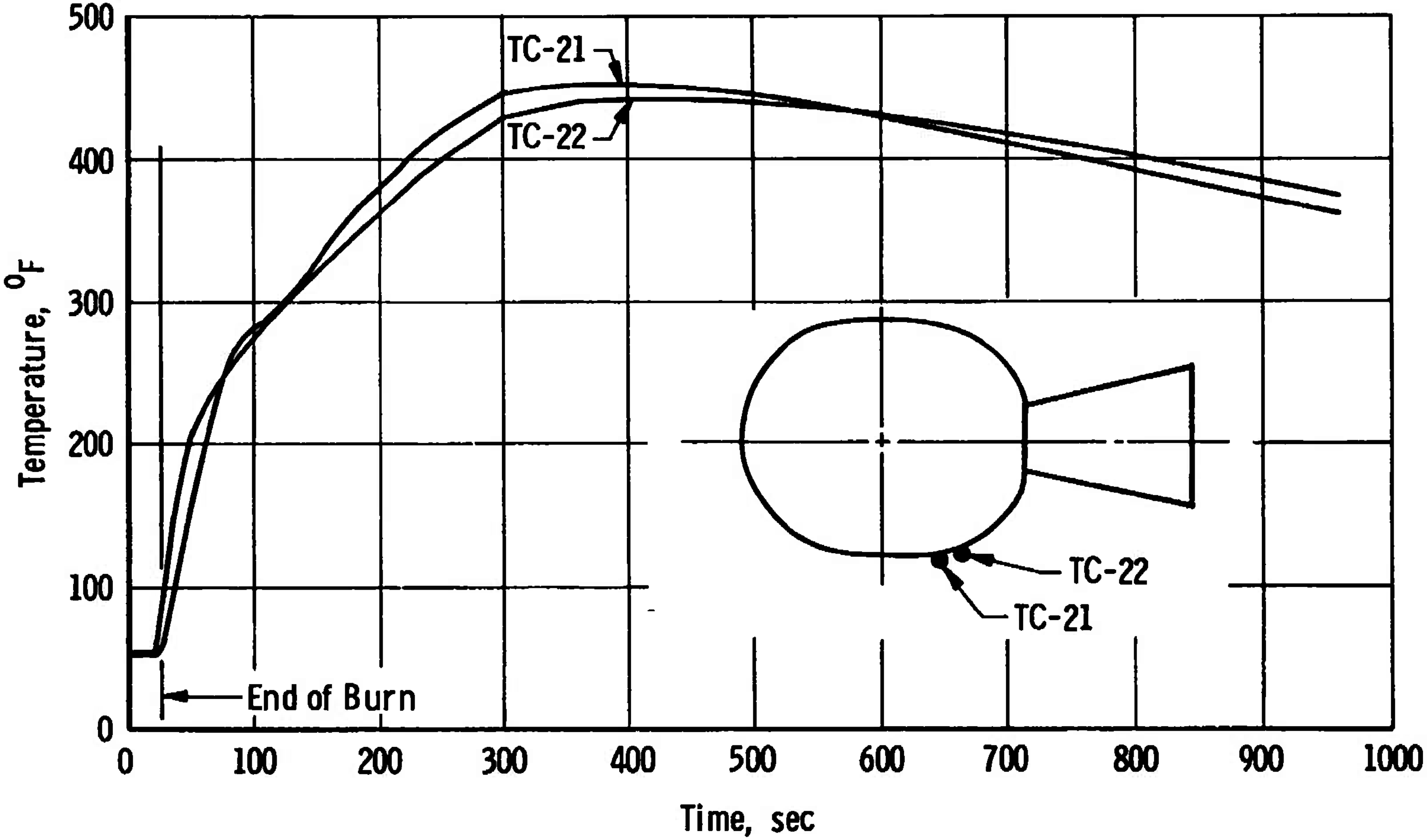

g. Motor Case; TC-21 and TC-22
Fig. 9 Continued

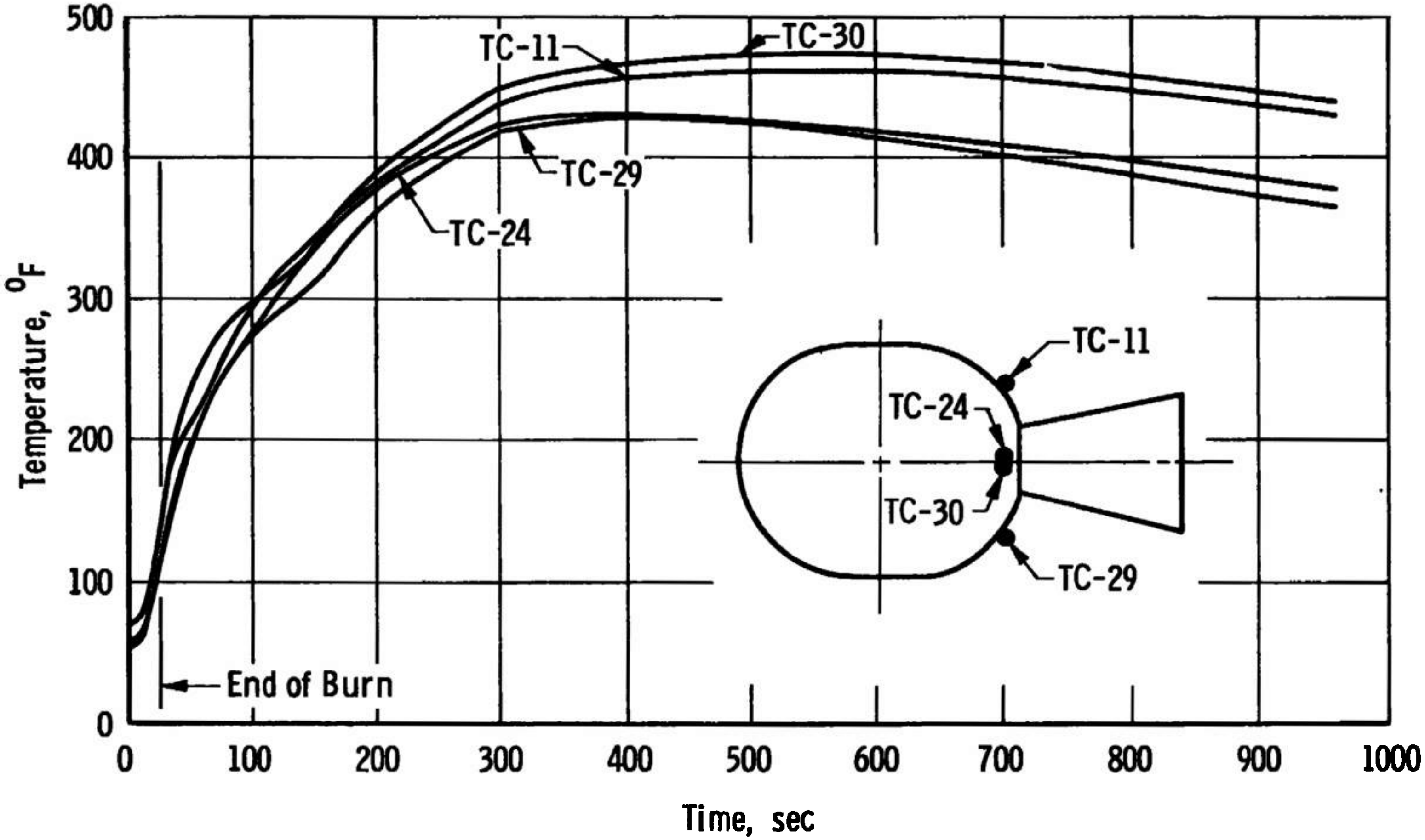

h. Motor Case; TC-11, TC-24, TC-29, and TC-30

Fig. 9 Continued

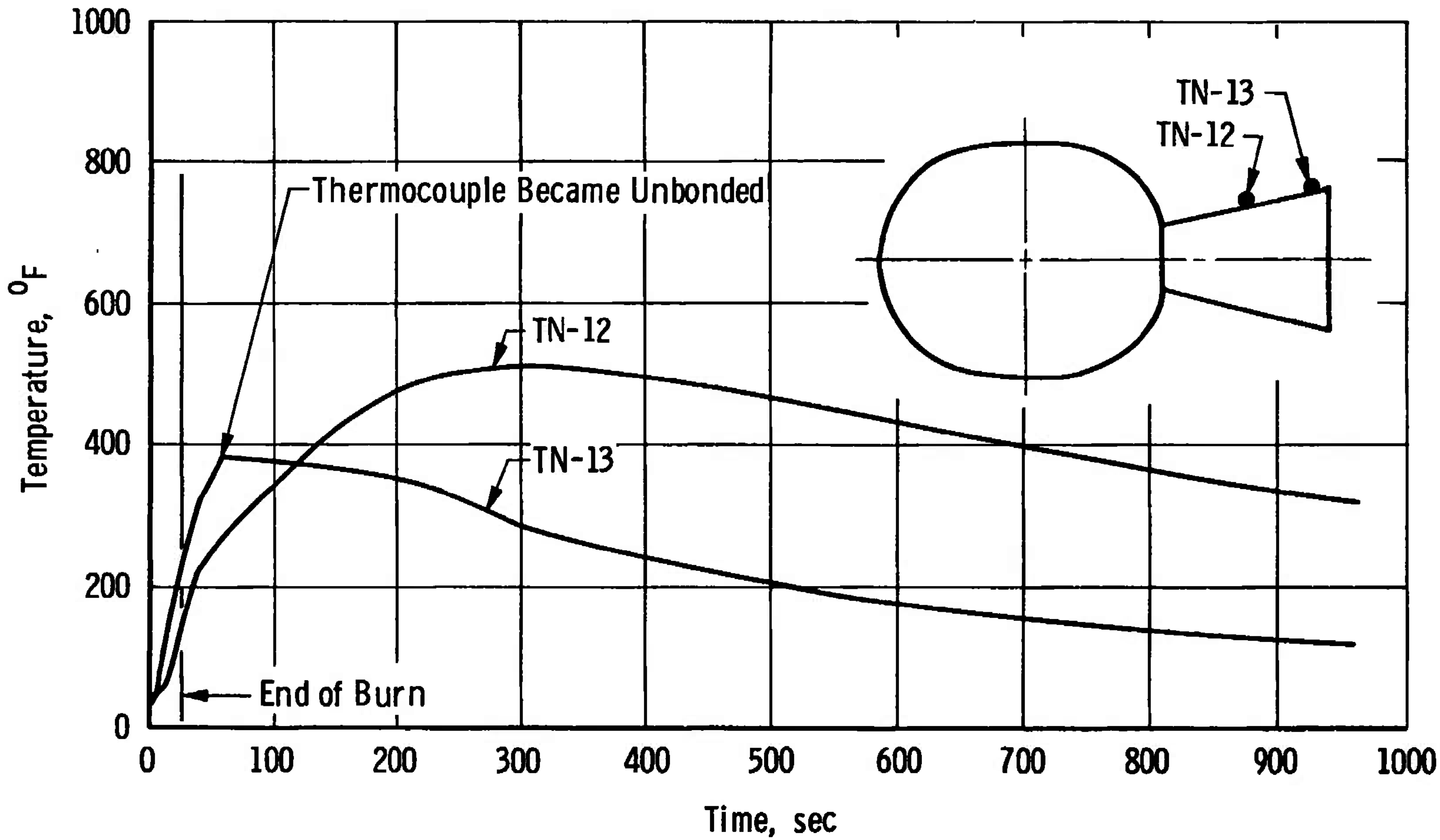

i. Nozzle; TN-12 and TN-13
Fig. 9 Continued

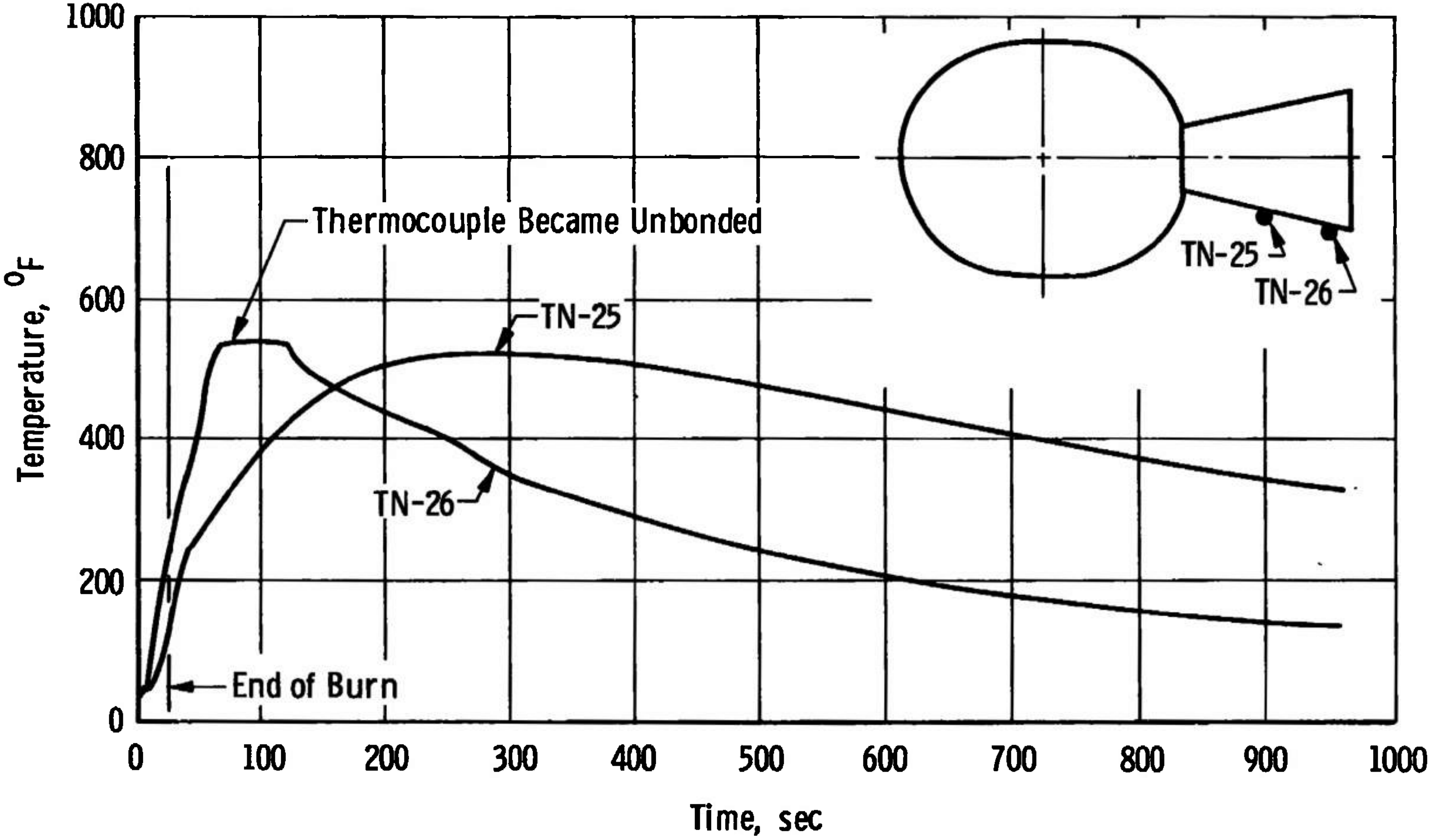

j. Nozzle; TN-25 and TN-26
Fig. 9 Continued

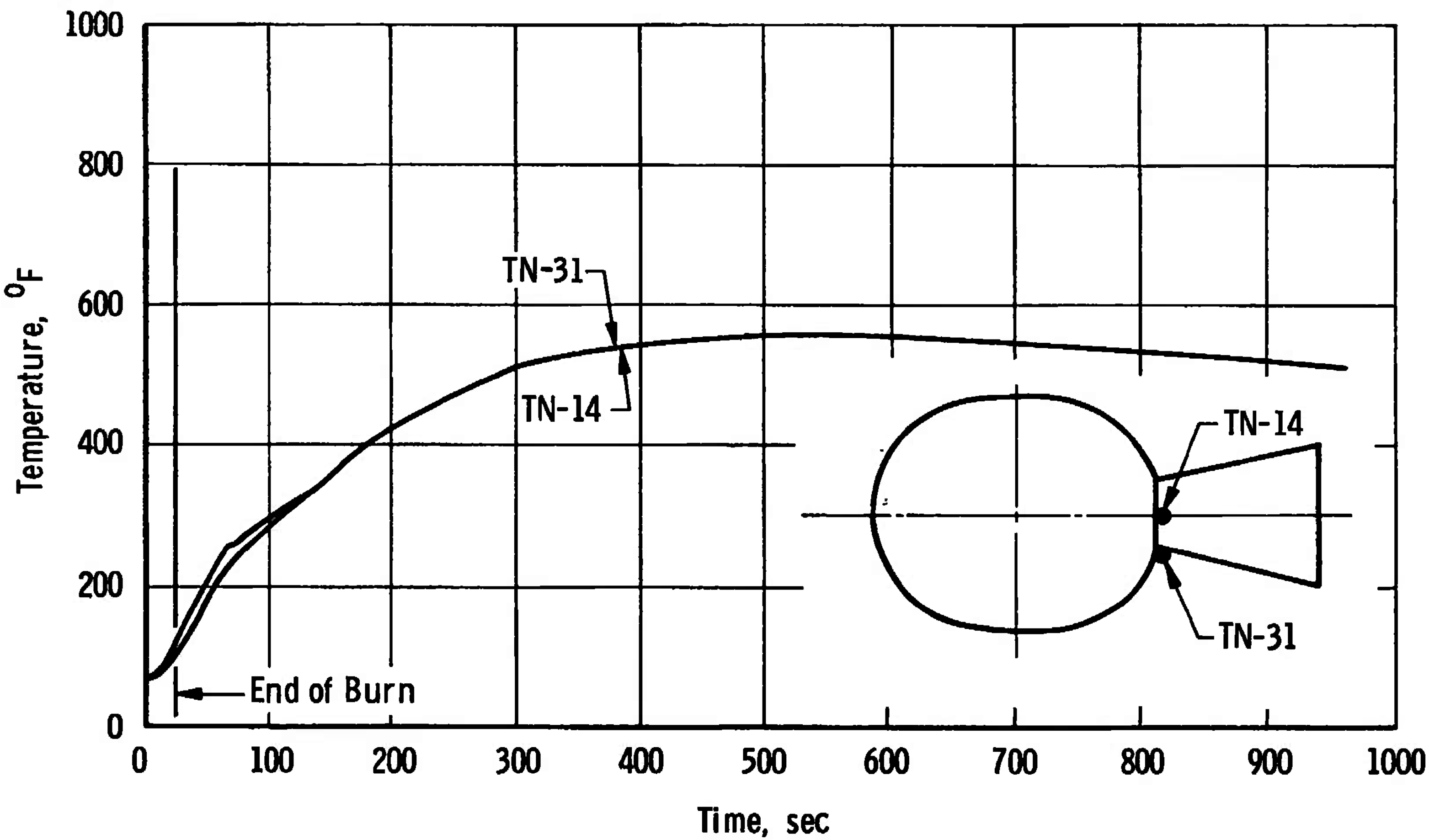

k. Nozzle; TN-14 and TN-31
Fig. 9 Concluded

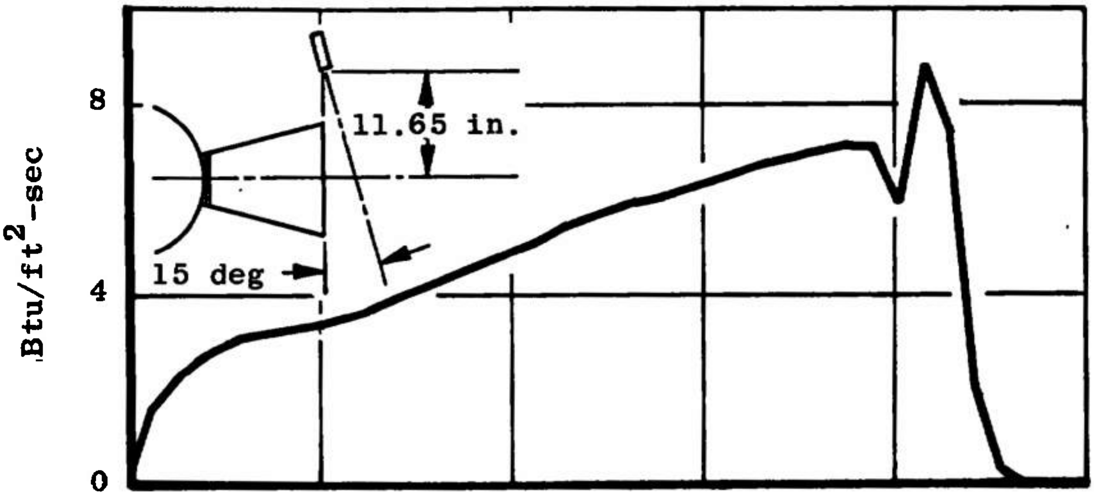

a. Radiometer, R-1 (View Angle = 30 deg)

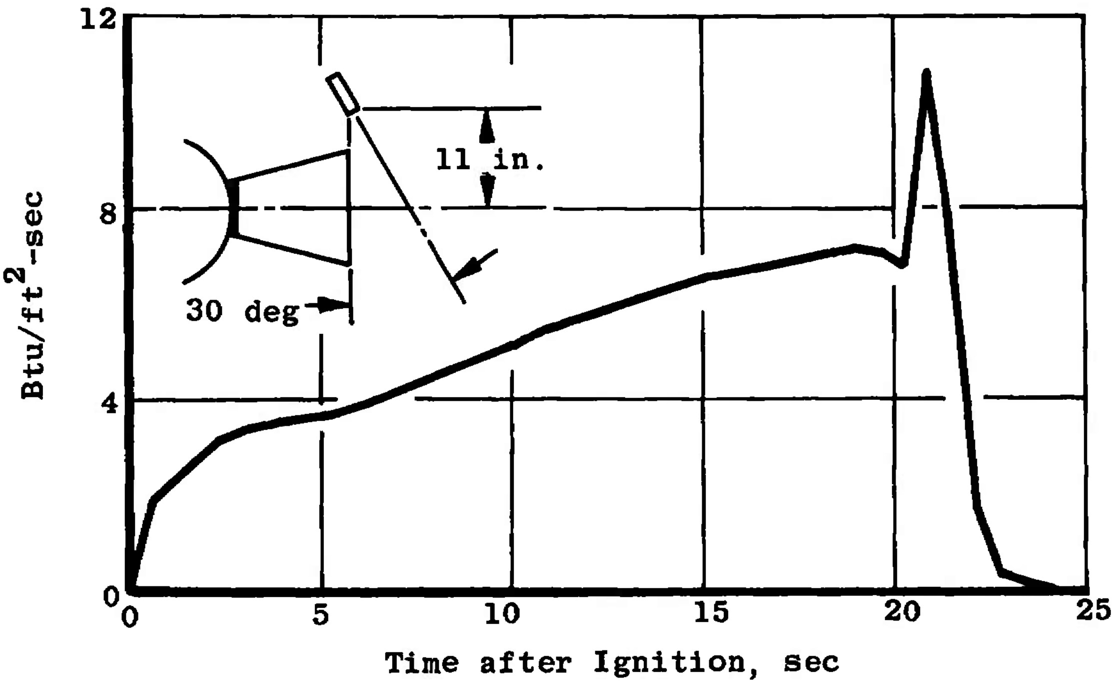

b. Radiometer, R-2 (View Angle = 60 deg)

Fig. 10 Exhaust Plume Radiation Variations with Time

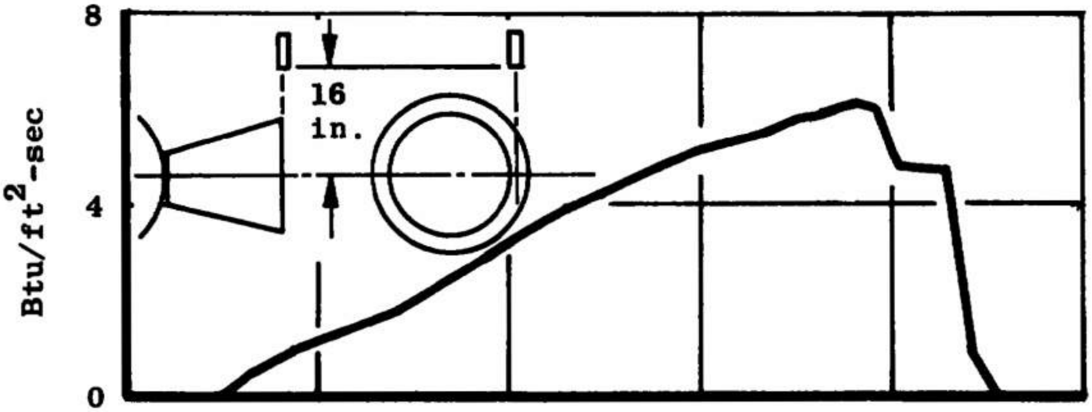

c. Radiometer, R-5 (View Angle = 3 deg)

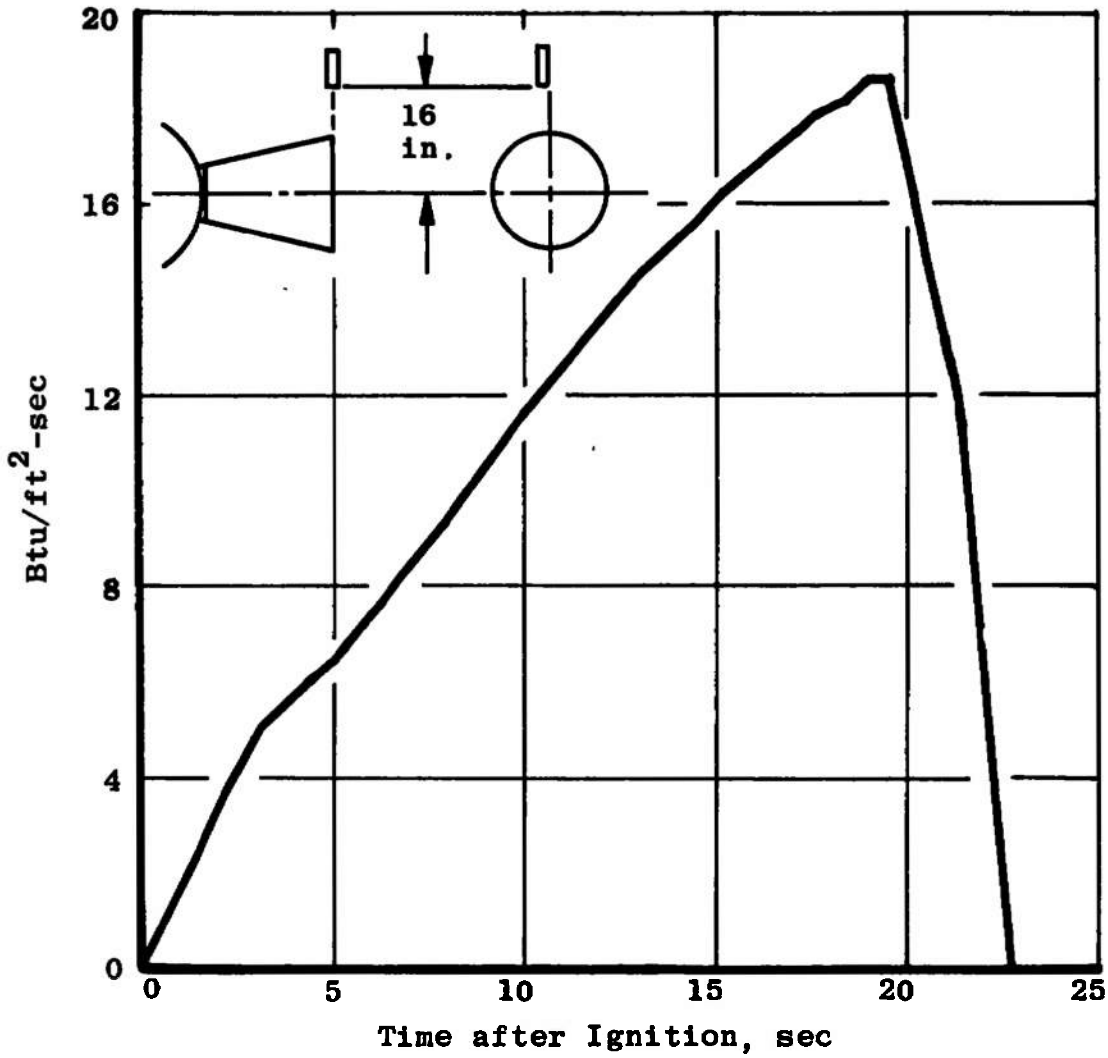

d. Radiometer, R-6 (View Angle = 3 deg)
Fig. 10 Concluded

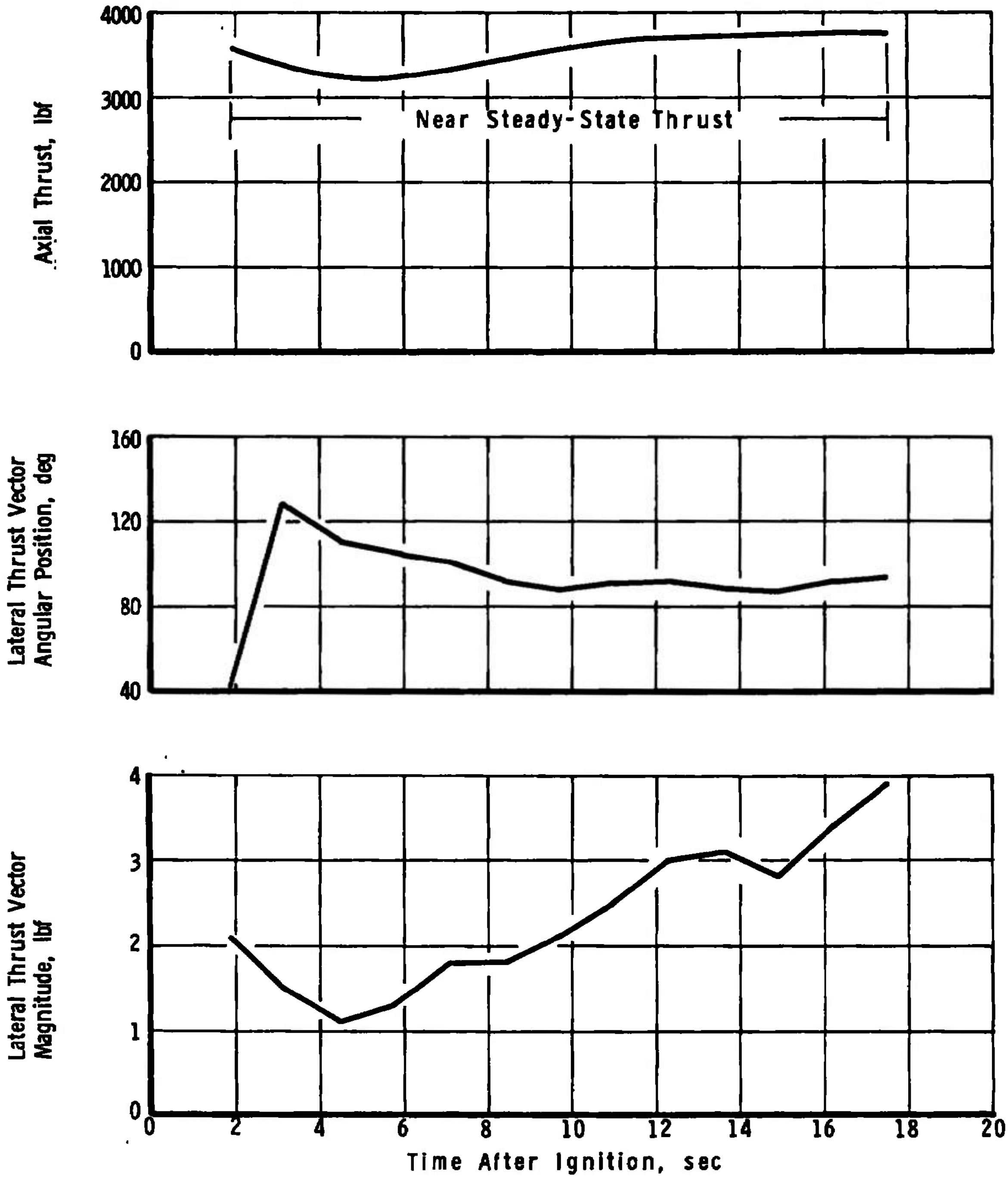

Fig. 11 Variation of Lateral Thrust Vector during Firing of TE-M-521-5 Motor S/N PV32-284-1

TABLE I
INSTRUMENTATION SUMMARY AND MEASUREMENT UNCERTAINTY

Parameter Designation	STEADY-STATE ESTIMATED MEASUREMENT*							Range	Type of Measuring Device	Type of Recording Device	Method of System Calibration
	Precision Index (S)			Bias (B)		Uncertainty ±(B + t_{95}S)					
	Percent of Reading	Unit of Measurement	Degrees of Freedom	Percent of Reading	Unit of Measurement	Percent of Reading	Unit of Measurement				
Axial Force, lbf	±0.13	---	198	±0.07	---	±0.33	---	3000 to 4000 lbf	Bonded Strain-Gage-Type Force Transducers	Voltage-to-Frequency Converter onto Magnetic Tape	In-Place Application of Deadweights Calibrated in the Standards Laboratory
Total Impulse, lbf-sec	±0.12	---	31	±0.07	---	±0.31	---				
Chamber Pressure, psia	±0.09	---	99	±0.07	---	±0.25	---	500 to 780 psia	Bonded Strain-Gage-Type Pressure Transducers		Resistance Shunt Based on the Standards Laboratory Determination of Transducer Applied Pressure versus Resistance Shunt Equivalent Pressure Relationship
Chamber Pressure Integral, psia-sec	±0.05	---	31	±0.07	---	±0.17	---				
Low-Range Chamber Pressure, psia	±(0.1% + 0.002 psi)		31		±0.008 psi	±(0.2% + 0.012 psi)		2.5 to 4 psia			
	±(0.1% + 0.002 psi)		31	±0.2	---	±(0.4% + 0.004 psi)		4 to 40 psia			
Test Cell Pressure, psia	±0.13	---	198	±1.50	---	±1.76	---	0.07 to 0.5 psia	Unbonded Strain-Gage-Type Pressure Transducers		
Test Cell Pressure Integral, psia-sec	±0.12	---	31	±1.50	---	±1.74	---				
Motor Temperature, °F	---	±0.25°F	95	---	±2.2°F	---	±2.7°F	0 to 600°F	Chromel-Alumel Temperature Transducers	Sequential Sampling, Millivolt-to-Digital Converter, and Magnetic Tape Storage Data Acquisition System	Millivolt Substitution Based on the NBS Temperature versus Millivolt Tables
Time Interval, msec	---	±0.25 msec	31	---	±0.01 msec	---	±0.5 msec	---	Time Pulse Generator	Photographically Recording Galvanometer Oscillograph	Time Pulse Generator Calibrated in the Standards Laboratory
Weight, lbf	---	±0.015 lbm	31	---	±0.02 lbm	---	±0.05 lbm	200 to 500 lbm	Beam-Balance Scales	Visual Readout	In-Place Application of Deadweights Calibrated in the Standards Laboratory
Lateral Thrust Vector Magnitude, lbf	---	±0.22 lbf	27	---	±0.39 lbf	---	±0.84 lbf	1 to 4 lbf	Bonded Strain-Gage-Type Force Transducers	Sequential Sampling, Millivolt-to-Digital Converter, and Magnetic Tape Storage Data Acquisition System	In-Place Application of Multiple Force Levels Measured with Force Transducers Calibrated in Standards Laboratory

*REFERENCE: CPIA No. 180, "ICRPG Handbook for Estimating the Uncertainty in Measurements Made with Liquid Propellant Rocket Engine Systems," April 30, 1969.

TABLE II
SUMMARY OF TE-M-521-5 MOTOR PERFORMANCE

Test Number	RA294	Ref. 2	Ref. 3
Motor Serial Number	PV32-284-1	PV32-222-48	PV32-248-2
Test Date	6-1-73	01-20-72	07-28-72
Average Motor Spin Rate during Firing, rpm	46	46	46
Prefire Conditioning Temperature (24 hr), °F	40	40	40
Motor Case Temperature at Ignition, °F	56	42	52
Number of Pyrogen Igniters Energized	1	2	2
Ignition Lag Time (t_ℓ), sec(1)	0.006	0.002	0.006
Ignition Time (t_i), sec(2)	0.185	——	0.110
Time from Ignition until Diffuser Flow Breakdowo (t_{bd}), sec	20.20	21.10	20.20
Action Time (t_a) sec (3)	20.60	21.26	20.68
Time Interval that Nozzle Throat Flow was Sonic (t_{is}), sec(4)	34.50	27.47	21.63
Simulated Altitude at Ignition, ft	117,000	121,000	115,000
Average Simulated Altitude during t_a, ft	103,000	108,000	108,000
Measured Total Impulse (Based on t_{bd}), lbf-sec			
Average of Four Channels of Data	70,644	70,801	70,831
Maximum Channel Deviation from Average, percent	0.030	0.024	0.040
Chambar Pressure Integral (Based on tbd), psia-sec			
Average of Two Channels of Data	13,100	13,214	13,072
Maximum Channel Deviation, percent	0.01	0.053	0.030
Cell Pressure Integral (Based on t_{bd}), psia-sec			
Average of Three Channels of Data	2.7144	2.3038	2.3628
Maximum Channel Deviation, percent	0.23	3.67	0.40
Vacuum Total Impulse (Based on t_a), lbf-sec	71,372	71,254	71,231
Vacuum Total Impulse (Based on t_{is}), lbf-sec	71,637	71,671	71,469
Vacuum Specific Impulse (Based on t_a), lbf-sec/lbm			
Based on the Manufacturer's Stated Propellant Weight	288.62	288.19	288.12
Based on Expended Mass (AEDC)	285 32	285.16	287.80
Vacuum Specific Impulse (Based on t_{is}), lbf-sec/lbm			
Basad on the Manufacturer's Stated Propellant Weight	289.69	289.81	289.08
Basad on Expended Mass (AEDC)	286.38	286.83	288.76
Average Vacuum Thrust Coefficient, C_F Based on t_a and Average Pre- and Postfire Areas	1.836	1.838	1.856

(1)Defined as the time interval from application of ignition voltage to the first perceptible rise in chamber pressure.

(2)Defined as the time interval from application of ignition voltage to attainment of 90 percent of peak thrust during the ignition transient.

(3)Defined as the time interval beginning when chamber pressure has risen to 10 percent of maximum at ignition and ending when chamber pressure has fallen to 10 percent of maximum during tailoff.

(4)Defined as the time interval between the first indication of chamber pressure at ignition and the time at which the ratio of chamber to cell pressure has decreased to 1.3 during tailoff.

TABLE III
SUMMARY OF TE-M-521-5 MOTOR PHYSICAL DIMENSIONS

Test Number	RA294	Ref. 2	Ref. 3
Motor Serial Number	PV32-284-1	PV32-222-48	PV32-248-2
Test Date	6/1/73	1/20/72	7/28/72
Motor Spin Rate, rpm	46	46	46
AEDC Prefire Motor Weight, lbm *	452.764	473.250	442.340
AEDC Postfire Motor Weight, lbm *	202.618	223.375	194.840
AEDC Expended Mass, lbm	250.146	249.875	247.500
Manufacturer's Stated Propellant Weight, lbm	247.29	247.30	247.2
Nozzle Throat Area, in.^{2}			
Prefire **	2.788	2.790	2.790
Postfire	3.113	3.076	3.082
Change from Prefire Measurement, percent	+11.7	+10.3	+10.5
Nozzle Exit Area, in.^{2}			
Prefire	149.234	148.41	148.53
Postfire	148.069	147.23	147.02
Change from Prefire Measurement, percent	-0.78	-0.8	-1.02

*Includes igniter weight and thrust adapter
**Supplied by motor manufacturer

UNCLASSIFIED

Security Classification

DOCUMENT CONTROL DATA - R & D

(Security classification of title, body of abstract and indexing annotation must be entered when the overall report is classified)

1. ORIGINATING ACTIVITY *(Corporate author)* Arnold Engineering Development Center, Arnold Air Force Station, Tennessee 37389	2a. REPORT SECURITY CLASSIFICATION UNCLASSIFIED 2b. GROUP N/A

3. REPORT TITLE

DESIGN ASSURANCE TEST OF THE THIOKOL TE-M-521-5 APOGEE KICK MOTOR TESTED IN THE SPIN MODE AT SIMULATED ALTITUDE CONDITIONS

4. DESCRIPTIVE NOTES *(Type of report and inclusive dates)*

June 1, 1973 - Final Report

5. AUTHOR(S) *(First name, middle initial, last name)*

J. O. Brooks and H. L. Merryman - ARO, Inc.

6. REPORT DATE	7a. TOTAL NO. OF PAGES	7b. NO. OF REFS
November 1973	49	5

8a. CONTRACT OR GRANT NO.	9a. ORIGINATOR'S REPORT NUMBER(S) AEDC-TR-73-170
b. PROJECT NO	
c. Program Element 921E3	9b. OTHER REPORT NO(S) *(Any other numbers that may be assigned this report)*
d.	ARO-ETF-TR-73-122

10. DISTRIBUTION STATEMENT

Approved for public release; distribution unlimited.

11. SUPPLEMENTARY NOTES	12. SPONSORING MILITARY ACTIVITY
Available in DDC.	NASA-GSFC Greenbelt, Maryland 20771

13. ABSTRACT

One Thiokol Chemical Corporation TE-M-521-5 solid-propellant rocket motor was successfully fired at an average simulated altitude of about 103,000 ft while spinning at 46 rpm. The general program objectives were to verify compliance of motor performance with the manufacturer's specifications. Specific primary objectives were to determine vacuum ballistic performance of the motor after prefire vibration conditioning and temperature conditioning at 40°F, altitude ignition characteristics, motor structural integrity, and motor temperature-time history during and after motor operation. Additional objectives were to measure the lateral (nonaxial) thrust component during motor operation and to measure radiation heat flux in the vicinity of the nozzle exit plane.

DD FORM 1 NOV 65 1473

UNCLASSIFIED

Security Classification

14. KEY WORDS	LINK A		LINK B		LINK C	
	ROLE	WT	ROLE	WT	ROLE	WT
rocket motor						
solid propellants						
space vehicle						
altitude simulation						
performance						
structural stability						
ignition						
ballistics						
spin stabilization						

AFSC
Arnold AFS Tenn